SIMULATION OF A NONLINEAR HYDRAULIC SYSTEM

N. SHASHA

A DISSERTATION

IN THE

FACULTY OF ENGINEERING

Presented in partial fulfilment of the requirements for the

Degree of MASTER OF ENGINEERING

at

Sir George Williams University

Montreal, Canada

Date: 21 September 1970.

ABSTRACT

In the design of control systems utilizing in part fluid power elements, classical methods of analysis become ineffective due to the many non linearities involved.

This dissertation considers the analysis and simulation of a hydraulic positional servo control system with an asymmetrical linear actuator forming part of the motion system of a six degrees of freedom flight simulator. A mathematical model is developed and simulated on an analog computer. The simulated results are compared with those obtained from the actual system under similar conditions.

It is established that this method yields satisfactory results in predicting the stability, the actuator displacement response and general trends in the system behaviour for step inputs.

However, deviations occur in the prediction of the maximum velocity and maximum error voltage, as indicated in section 4.4.

Factors causing some of these deviations and future improvements in the simulation are discussed in chapter 5.

ACKNOWLEDGEMENT

The author wishes to express his gratitude to his advisor Dr. G.K. Fleming for the suggestions and assistance given throughout the dissertation. In addition he wishes to thank Dr. M. duPlessis and Dr. G. Mueller for their most helpful comments.

A note of acknowledgement is due to the author's colleagues at CAE who helped in the system test and recordings. Finally, the author is indebted to Mr. D.R. Tait for his support of this work.

TABLE OF CONTENTS

LIST OF FIGURES

Chapter 1

INTRODUCTION

1.1 Motivation

In Control Systems utilizing hydraulic power such as the motion system of a flight simulator the dynamics of the hydraulic part are the dominant factor in determining the performance of the whole system. However they are difficult to analyse due to the inherent non linearities. It became desirable to develop a representative mathematical model of the hydraulic control system in order to enable analysis of its performance through simulation. This can help in predicting the system behaviour and optimizing its performance in early design stages, prior to its physical construction thus obviating the need for building prototypes and saving cost and time in later modifications and adjustments.

This was the primary motivation which resulted in the work described in this dissertation.

1.2 Review of Literature

The study of hydraulic control systems from an analytical point of view received little attention prior to 1950. All the material on hydraulic systems published until that time was of a descriptive or empirical nature.

The first attempts to analyse hydraulic systems especially since the increased use of electro hydraulic servo valves were done utilizing existing techniques for solving electrical systems.

The emphasis was to represent the hydraulic system as a linear model, simplified to allow its solution.

The first contributions to a study of hydraulic systems were the products of Dynamic Analysis and Control Laboratory (DACL) at the Massachusett's Institute of Technology. LEE AND BLACKBURN (1-6) produced a series of six papers between 1951 and 1954 entitled "Contributions to Hydraulic Control" in which they discussed the work done at the DACL.

This work involved studies of the flow forces on spool valves, spool redesign to compensate for these forces, valve instabilities and hydraulic network analysis. In appendix "A" of this dissertation these forces are further discussed and the analysis is adapted to the particular type of valve used in the system studied in this dissertation.

The work of LEE AND BLACKBURN together with the work done by SHEARER (8) as well as subsequent work done by these and others was published in a book (7) in 1960.

The limitations of linearized models are discussed by RAUSCH (9) who developed a non linear model of a positional hydraulic control system. The assumption of uniform pressure distribution throughout the control volume was discussed and forms the basis of the same assumption in this paper.

G. K. FLEMING (10) studied the oscillations of an actual hydraulic positional control system with mechanical feedback, developed its mathematical model and discussed its inherent non linearities. A detailed analysis of jet attachment phenomena in spool valves and their effect on system instability was presented.

FITCH (11) discussed a model including the spool forces in a mechanical feedback hydraulic system emphasizing the effect of the spool position on the system equations as applicable for analog simulation. SINH (12) compared the results obtained from an experimental velocity control hydraulic system consisting basically of an electro hydraulic valve controlled motor with the results from the simulation of the same system. This was a major step in verifying the accuracy of the mathematical model and of the simulation techniques. GLICKMAN (13) presented a detailed block diagram for hydraulic control systems with linear actuators.

WANG (14) developed a mathematical model for an electro hydraul-

ic valve - controlled actuators emphasizing the time-domain trajectories for various types of inputs and compared the results solved on an analog computer with the results from an actual system. The actuator in this system was symmetrical but the approach to the problem deviated from others in that the pressures in each chamber were calculated separately and not lumped into a load pressure drop.

Other works of major contribution to this field is presented in (15) to (20).

1.3 Object of Study

The object of the present work is to derive a mathematical model for the hydraulic system of the motion platform of a six degrees of freedom flight simulator. The hydraulic system is one block in the overall complex control system but its behaviour under various conditions as encountered in flight simulator operation could not be predicted with reasonable accuracy prior to their actual operation. As indicated in the last section much effort has been invested in developing mathematical models of hydraulic systems. Only few of the theoretical analyses have been verified by experimental work. Also, the case of an asymmetrical linear actuator used in the motion system of the flight simulator was not dealt with previously.

Effects of parameters such as spool steady state and transient flow forces and changing chamber volumes are investigated.

With a representative mathematical model the system could be studied through simulation and slowing it by time scaling allows careful scrutiny of its transients. By varying the parameters through their possible ranges improvements could be made in the design stages, allowing their selection for optimization of total system performance under the various conditions of operation predicted.

The system is described in chapter 2 and its mathematical model derived in chapter 3.

Chapter 2

SYSTEM DESCRIPTION

2.1 Introduction

The system considered forms the basic part of the motion system of a flight simulator consisting of a cockpit and a motion platform mounted on six linear actuators arranged in three pairs of inverted V's to enable movement of the platform in six degrees of freedom. Each linear actuator forms part of an independent closed loop control system. The input signals to this system are analog converted commands from a digital computer which coordinates cockpit motion in accordance with prevailing simulated flight conditions and pilot's commands.

Henceforth the system to be dealt with will be one of the six individual control systems shown schematically in Figure 2-1, page 12 consisting of an asymmetrical linear actuator controlled by an electro hydraulic servo valve manifold mounted on the actuator together with other associated valves.

The system hydraulic pressure supply is provided by a variable displacement, pressure compensated, axial piston pump feeding a battery of six accumulators connected in parallel. Fluid from the accumulators is distributed to the six control systems via a

pressure loop and micronic filters. The fluid enters the 4 way electro hydraulic servo valve which controls the flow to and from the linear actuator. A pressure relief valve in each line to the actuator limits the maximum pressure that can develop in the actuator rod end and head end chambers to a safe limit based on mechanical considerations yet higher than the value of the system pressure. A replenishing check valve installed in each line and connected to the return manifold prevents cavitation in the actuator chambers as can occur during high deceleration periods.

To the piston rod a rotary potentiometer is connected via a precision rack and pinion arrangement which monitors the actuator extension and closes the loop by feeding a voltage to a summing junction and subtracting it from the input signal voltage. The error voltage thus resulting passes through an RC network and an amplifier. The RC network reduces the rate of voltage variation providing a smooth input to the valve torque motor which is essential to the performance of the motion system of a flight simulator. The current to the valve is then limited by a resistor in the line from the amplifier to the valve.

A mechanical deceleration valve is installed at each actuator chamber and is operational at the extreme ends of travel only. The actuator is a sealed piston type double acting cylinder with

a piston rod on one side only. It is pivoted at its lower end to the base and connected at the (upper) piston rod end to a rotating joint at the motion platform supporting its portion of the cockpit and platform weight.

The return lines from the six control systems feed into a common return loop which directs the fluid to the oil reservoir. The oil in the reservoir is continuously filtered and cooled through a thermostat regulated heat exchanger which maintains the fluid temperature within a close range after a certain start up period.

2.2 Operation of the System

The fluid supplied to the system enters the pressure port of the electro hydraulic servo valve and depending on its main spool position the fluid is directed to either one of the outlet ports or prevented from passing. If fluid passes out of one outlet port then the other outlet port will be connected to the return line.

Thus the position of the main spool controls the direction and amount of flow to the actuator and hence the actuator will extend, retract or remain in its position depending on the corresponding valve main spool position.

The actuator's piston rod, being on one side only, reduces the

effective area on the rod end side and hence the areas on each side of the piston are unequal and have a ratio of 1:2. 44 causing an unbalance in the flow to and from the actuator.

The electro hydraulic servo valve is a two stage 4 way critical center spool valve and is a two stage 4 way critical center spool valve and is a MOOG 72 series force feed back type. Its operation is indicated schematically in figures 2-2 and 2-3. It consists of a polarized electrical torque motor and two stages of hydraulic power amplification. The motor armature extends into the air gaps of the magnetic flux circuit and is supported in this position by a flexure tube member. The two motor coils surround the armature, one on each side of the flexure tube.

The flapper of the first stage hydraulic amplifier is rigidly attached to the midpoint of the armature. The flapper extends through the flexure tube and passes between two nozzles, creating two variable orifices between the nozzle tips and the flapper. The pressure controlled by the flapper and nozzle variable orifice is fed to the end areas of the second stage (main) spool.

A cantilever feedback spring is fixed to the flapper and engages a slot at the center of the spool. Displacement of the spool deflects the feedback spring which creates a torque on the armature/flapper assembly.

Input signal induces a magnetic charge in the armature and causes a deflection of the armature and flapper. This assembly pivots about the flexure tube and varies the nozzle downstream back pressure increasing it on one side and decreasing it on the other.

This action creates a differential pressure from one end of the spool to the other and results in spool displacement. The spool displacement causes a torque in the feedback wire which opposes the original input signal torque. Spool movement continues until the feedback wire torque equals the input signal torque.

As mentioned earlier rapidly decelerated motions can induce cavitation in the actuator chamber. In this case the replenishing check valve opens and allows fluid from the return manifold to enter the cavitating chamber.

As the simulation of the system deals with the normal operational excursions of the system which do not include the extremes of actuator travel, the effect of the deceleration valve is not included in the model. Figure 2-4 shows a simplified block diagram of the system.

In chapter 3 the mathematical model for the system described

above is derived with the basic assumptions made for this type of systems as found in the literature mentioned in chapter 1 and developed further in chapter 3.

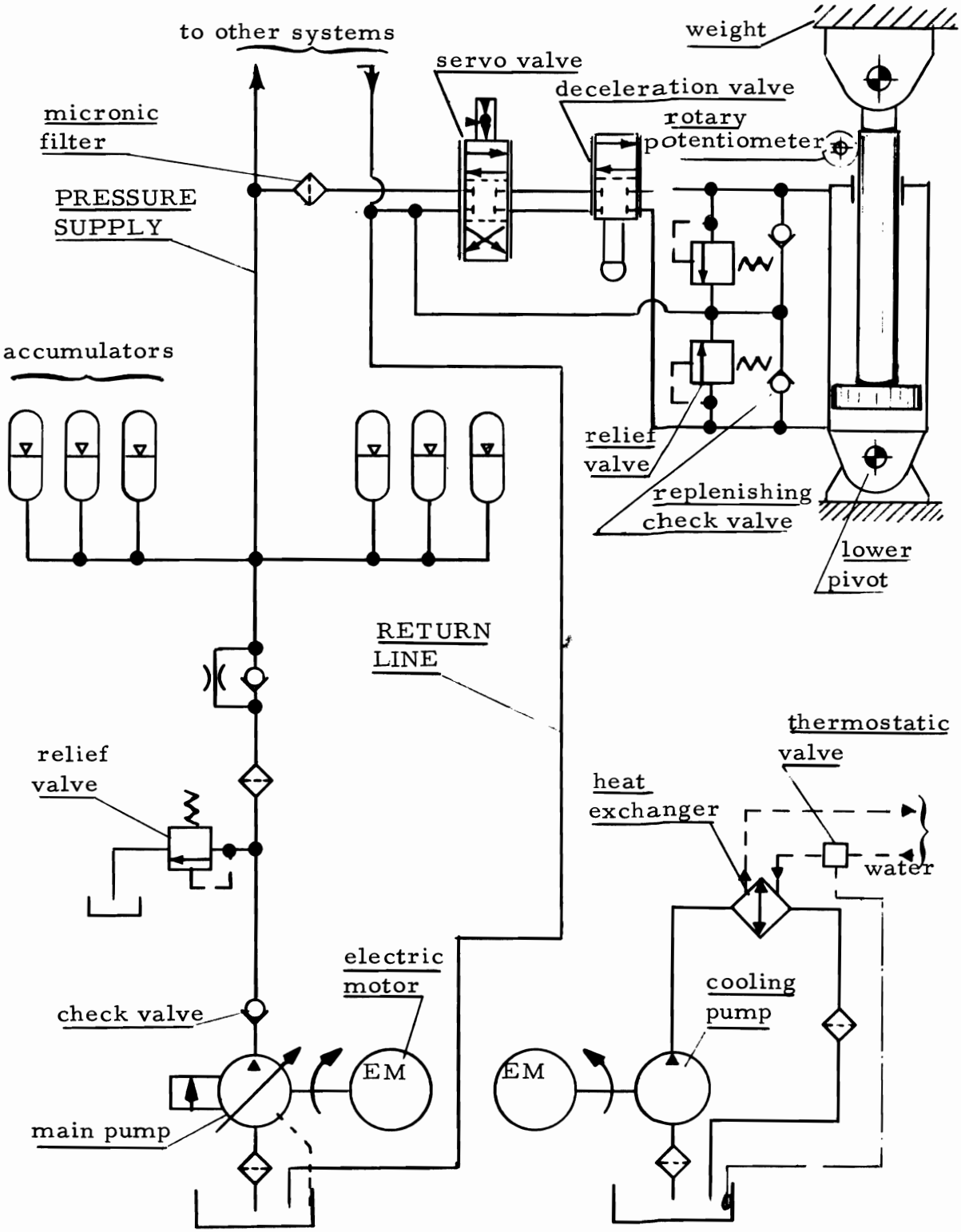

Figure 2-1 System Schematic

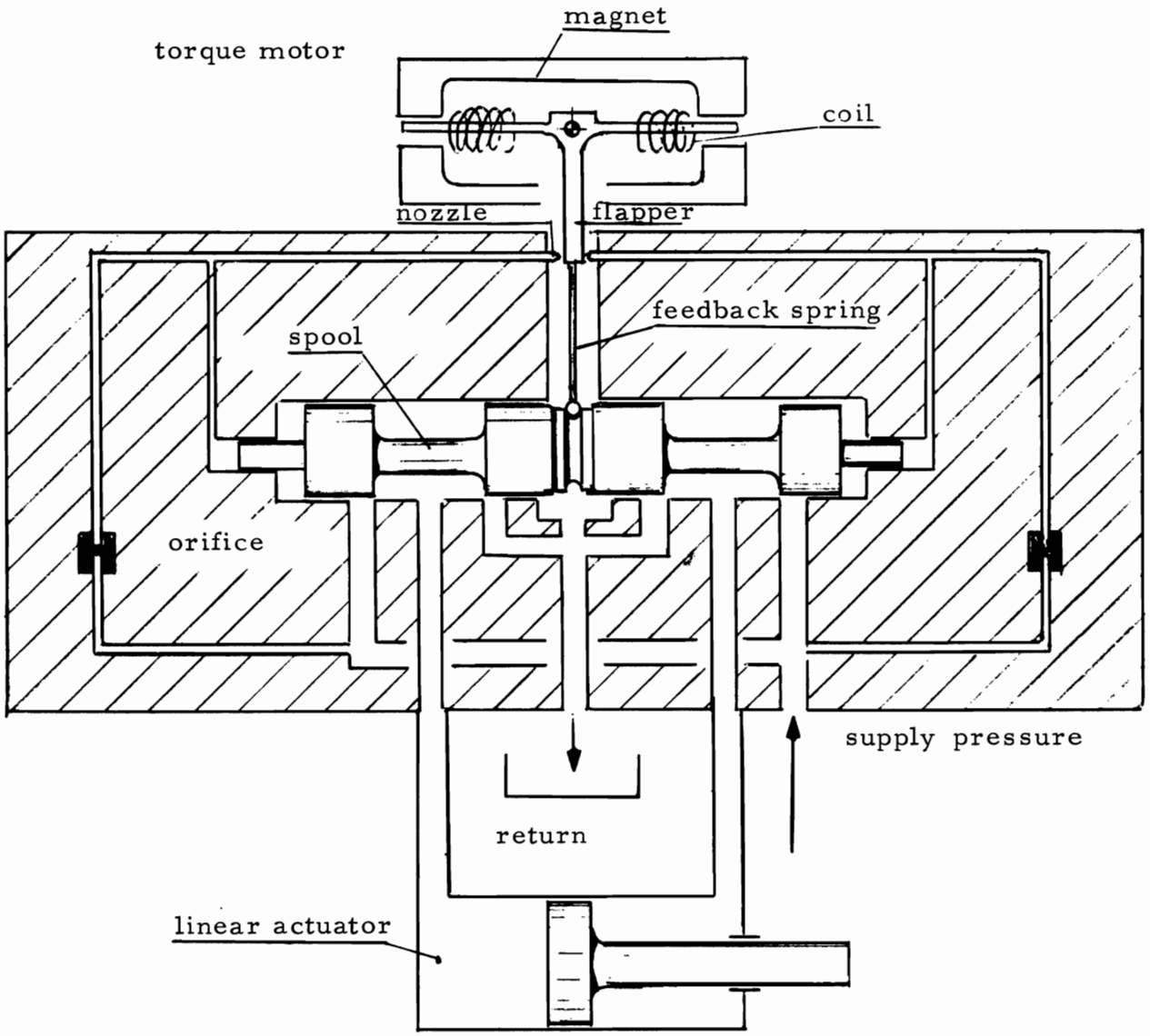

Figure 2-2 Servo Valve Schematic (Neutral Position)

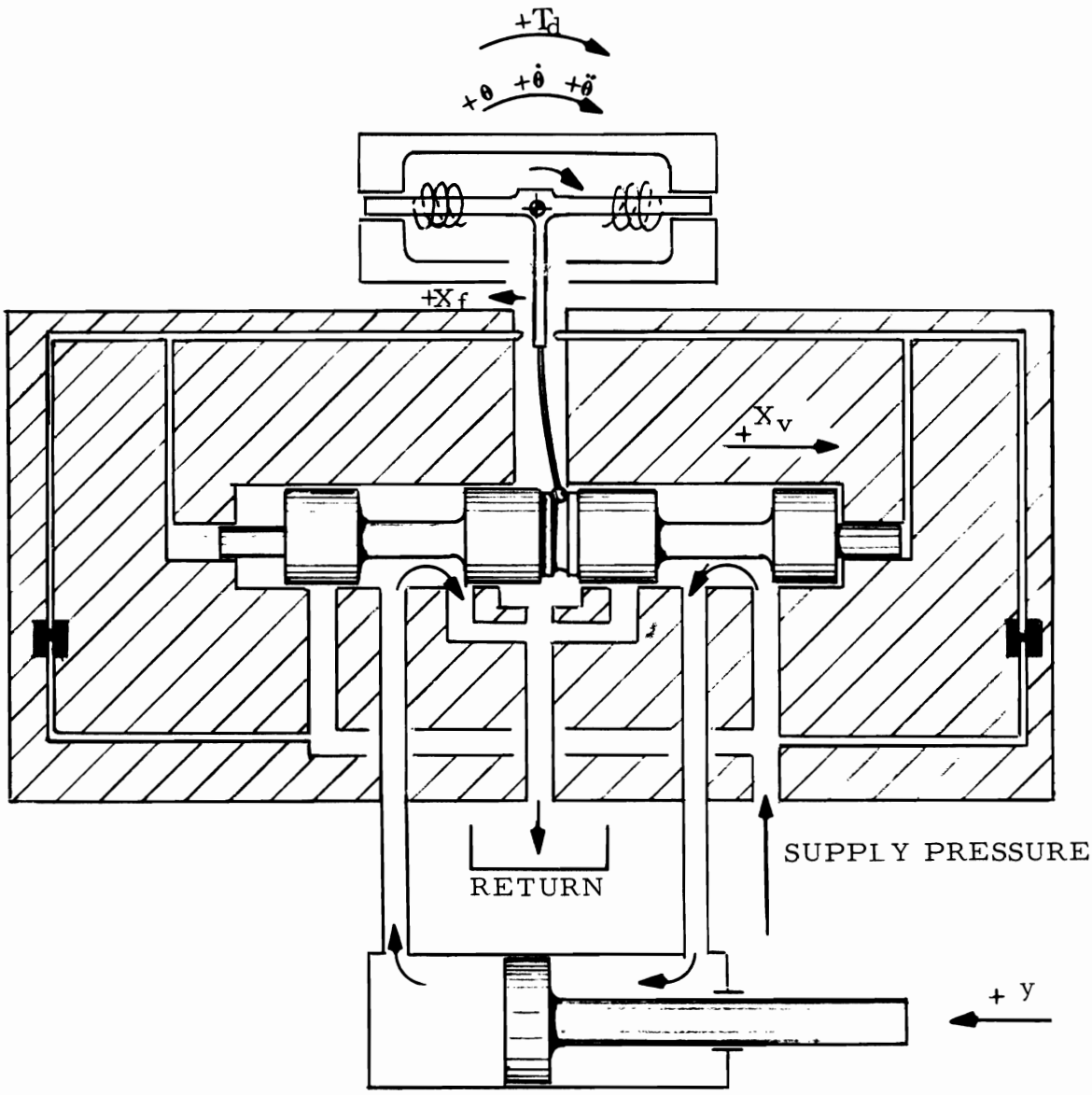

Figure 2-3 Servo Valve Schematic (Operating Position)

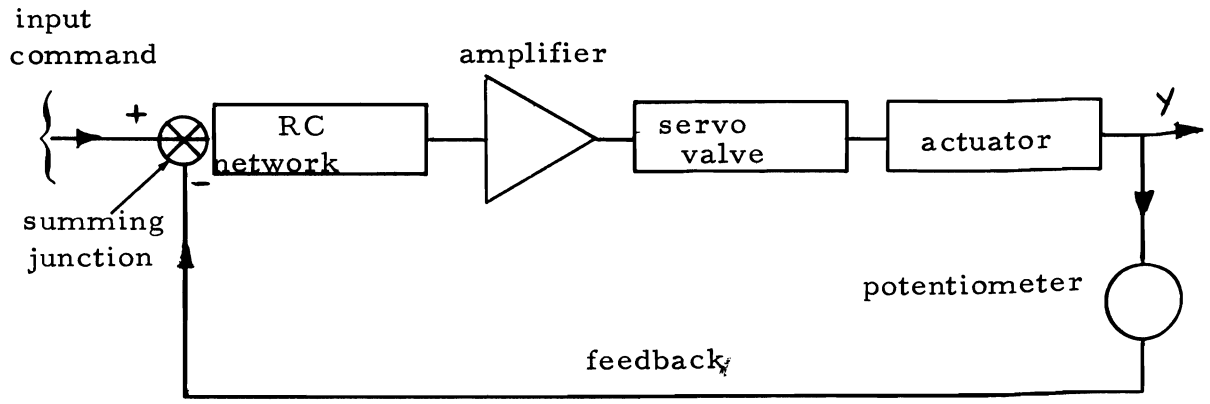

Figure 2-4 System Block Diagram

Chapter 3

MATHEMATICAL MODEL OF THE SYSTEM

3.1 Introduction

This chapter will be mainly devoted to the derivation and summarization of the equations representing the mathematical model of the system described in chapter 2.

In trying to keep the model as simple as possible to enable its effective use for evaluation purposes without degrading the accuracy of system performance prediction from the model, studies were made to determine the effect of some of the variables such as flow forces and changing volumes on the system performance and these were dropped from the model when their contribution was insignificant. Also non linearities were removed from the model wherever their effects on the system performance were negligible.

Some basic assumptions are made in deriving the equations and these are as follows:

(1) The hydraulic fluid is compressible within the actuator chambers while the fluid flow through the pipes and valves is considered as ideal (23).

(2) The pressure is distributed uniformly within each separate actuator chamber and piping, (9).

(3) The hydraulic pump and accumulators are not simulated; rather, a constant supply pressure is used. The sizing of the accumulators is such that under normal excursions little drop in pressure occurs in the supply line.

(4) The temperature of the fluid is uniform throughout the system and does not vary with time. Based on this assumption both the bulk modulus of elasticity and the density of the fluid are assumed constant, (10).

(5) The flow resistance in the tubing, manifolds and the fully open deceleration valve has been calculated and found negligible compared with the resistance in the control valve orifices.

(6) Return line pressure is considered to be atmospheric. Pressure measurements in the return line at maximum flow conditions indicated negligible values as compared with system pressure.

(7) The valve has critical center spool, i. e., the spool lands are perfectly matched and there is no underlap or overlap.

(8) The coulomb friction in the actuator and the valve spool is negligible, (10).

(9) The fluid inertance is neglected, (10).

(10) The valve flow-displacement hysteresis is neglected, (10).

Further assumptions will be made in the following sections as the model of each main component of the system is derived.

The definition of the symbols used is detailed in appendix "E".

3.2 Mathematical Model Development

At this stage a sign convention is defined for the system which applies to all its components. This is shown in figure 2-3, page 14.

A positive current causes a clockwise rotation of the torque motor which will be assumed positive direction of θ. This in turn will cause a positive displacement of the flapper x_f to the left building up pressure in the left hand spool chamber and causing the main spool to displace in the positive direction, to the right. This in turn will cause the actuator to retract and hence the direction of retraction will be the positive y direction.

This sign convention will prove useful and essential in investigating spool forces and the effects of spool movement.

In the following sections the model of each component of the system is derived and the total system model is obtained from the individual models of its components.

3.2.1 Servo Valve Model

The servo valve was described in section 2-2 and shown in figures 2-2 and 2-3. Obviously the valve has many inherent nonlinearities and some work was done (21) to include these in the model raising the order of the transfer function to 8. Unfortunately these complex analysis have not contributed significantly to servo valve design due to uncertainties and inaccuracies associated with the higher order effects. These analyses, however, have been extremely useful when reduced to their simpler form.

The following assumptions are made:

(1) Motions of the flapper are small with respect to spool position.

(2) The forces acting on the flapper are negligible.

3.2.1.1 Torque Motor

The torque motor was rigorously analysed by Merritt (22) who summarized the torque developed by the entry current as:

$$T_d = K_1 I_s + K_m \theta \quad \ldots\ldots (3\text{-}1)$$

where the angle of rotation induces higher torque due to the decrease in magnetic resistance. Applying Newton's second law to the armature, we get:

$$T_d = J_a \frac{d^2\theta}{dt^2} + B_a \frac{d\theta}{dt} + K_a \theta + K_w (x_f + x_v) \quad \ldots\ldots (3\text{-}2)$$

θ being very small we can write:

$$\frac{x_f}{r} = \tan \theta \approx \theta \quad \ldots\ldots (3\text{-}3)$$

and as per assumption (1) $x_f << x_v$ $\ldots\ldots (3\text{-}4)$

combining equations 3-1 to 3-4 we get:

$$T_d = \frac{J_a}{r} \frac{d^2\theta}{dt^2} + \frac{B_a}{r} \frac{d\theta}{dt} + \frac{K_a}{r} \theta + K_w (x_f + x_v) \quad \ldots (3\text{-}5)$$

designating,

$$J_f = \frac{J_a}{r}, \quad B_f = \frac{B_a}{r}, \quad K_f = \frac{K_a - K_m}{r}$$

equation 3-5 becomes:

$$K_1 I_s - K_w X_v = J_f \frac{d^2 x_f}{dt^2} + B_f \frac{dx_f}{dt} + K_f x_f \quad \ldots\ldots (3\text{-}6)$$

The form of (3-6) used in the analog simulation will be:

$$\ddot{x}_f = -2\omega_n \zeta_n \dot{x}_f - \omega_n^2 x_f + \frac{K_1 \omega^2_n}{K_f} I_s - \frac{K_w}{K_f} \omega_n^2 x_v \quad \ldots (3\text{-}7)$$

where $\omega_n = \sqrt{\frac{K_f}{J_f}}$, $\zeta_n = \frac{1}{2} \frac{B_f \dot{\omega}_n}{K_f}$

The Laplace transform of (3-6) used in linear analysis is:

$$\frac{x_f}{K_1 I_s - K_w x_v} = \frac{1/K_f}{\left(\frac{s}{\omega_n}\right)^2 + \frac{2\zeta_n}{\omega_n} s + 1}$$

where ω_n and ζ_n are as defined above.

3.2.1.2 First Stage Model

The Flapper-spool relationship is investigated next.

The force balance across the main spool can be written as:

$$A_v P_{Lv} = M_v \ddot{x}_v + .43\, w (P_s - P_L) X_v \pm C_d \sqrt{2\rho}\, w \Delta L \sqrt{\Delta p}\, \dot{x}_v$$

The second and third terms are the steady state and transient flow forces respectively and are derived in Appendix "A" together with an explanation of the sign of the third term.

Merritt (22) justifies the linearization of the flapper nozzle flow equation which is defined as follows:

$$Q_{Lv} = K_2 x_f - K_{c_p} P_{L_v} \quad \ldots\ldots (3\text{-}10)$$

Also

$$Q_{Lv} = \frac{Vv}{4\beta} \cdot \frac{dP_{Lv}}{dt} + C_{t_s} P_{L_v} + A_v \dot{x}_v \quad \ldots.(3\text{-}11)$$

as explained in appendix "B".

Combining (3-10) and (3-11) and taking the Laplace Transform we get:

$$P_{Lv}\left(K_{ce} + \frac{V_v}{4\beta} \cdot s\right) = K_2 x_f - A_v \cdot s x_v \quad \ldots..(3\text{-}12)$$

where $K_{ce} = K_{cp} + C_{t_s}$

combining (3-12) and (3-9) and taking the Laplace Transform we get:

$$X_v = \frac{\dfrac{A_v K_2 x_f}{K_{ce} + \dfrac{V_v}{4\beta} \cdot s}}{M_v S^2 + \dfrac{A_v^2}{K_{ce} + \dfrac{V_v}{4\beta} \cdot s} \pm C_d\sqrt{2\rho}\, w \Delta L \sqrt{\Delta p}. s + .43 w(P_s - P_L)} \quad \ldots.(3\text{-}13)$$

designating

$$\omega_h = \sqrt{\frac{4\beta \cdot A_v^2}{M_v \cdot V_v}}, \quad \delta_h = \frac{\omega_n K_{ce} M_v}{2 A_v^2}$$

$$D = C_d\sqrt{2\rho}\, w \Delta L \sqrt{\Delta p}, \quad E = .43 w(P_s - P_L)$$

and after some algebraic manipulations we get:

$$X_v = \frac{\dfrac{K_2}{A_v} x_f}{\dfrac{S^3}{\omega_h^2} + \left(\dfrac{2\delta_h}{\omega_h} \pm \dfrac{D}{\omega_h^2 M_v}\right)S^2 + \left(\pm \dfrac{DK_{ce}}{A_v^2} + \dfrac{E \cdot V_v}{4\beta} + 1\right)S + \dfrac{EK_{ce}}{A_v^2}} \quad \ldots(3\text{-}14)$$

Writing (3-14) in the form used for analog computers we get:

$$\dddot{X}_v = \frac{K_2}{A_v}\omega_h^2 x_f - \left(2\delta_h\omega_h \pm \frac{D}{M_v}\right)\ddot{x}_v - \omega_h^2\left(\frac{\pm DK_{ce}}{A_v^2} + \frac{E.V_v}{4\beta} + 1\right)\dot{x}_v - \frac{EK_{ce}}{A_v^2}$$

.....(3-15)

An investigation into the effect of the flow forces terms D and E was conducted and found negligible as explained in Appendix "A". Hence by neglecting these terms (3-15) becomes

$$\dddot{X}_v = \frac{K_2}{A_v}\omega_h^2 x_f - 2\delta_h\omega_h \ddot{x}_v - \omega_h^2 \dot{x}_v \qquad .....(3-16)$$

(3-16) will be used in the final system simulation.

This equation will be valid whether the load is symmetrical as with a hydraulic motor or asymmetrical as with the case investigated of a hydraulic linear actuator with different areas.

3.2.2 Second Stage and Load Model

The valve second stage main spool and linear actuator relationship will be developed in this section.

Figure 3-1 shows the flow directions for main spool displacement to the right i. e. positive Xv. We have from Appendix "B", applying the continuity equation to the rod end side.

$$Q_1 = A_1 \cdot \dot{y} + \frac{V_{t_1} + A_1 y}{\beta}\dot{P}_1 + C_\ell(P_1 - P_2) \qquad .... (3-17)$$

y is taken to be zero at mid stroke of the actuator.

The leakage flow $C_\ell(P1 - P2)$ is assumed to lump the leakages across the actuator, the spool and other valves in the system to simplify the representation.

Also by considering the spool opening as an orifice with constant discharge coefficient C_d and area $w.X_v$ we get:

$$Q_1 = \sqrt{\frac{2}{\rho}}\ C_d\, w.X_v \sqrt{P_s - P_1} \qquad \ldots\ldots\ldots (3\text{-}18)$$

Similarily, considering the flow continuity equation for the full end side we get:

$$Q_2 = A_2 \cdot \dot{y} - \frac{V_{t2} - A_{2.y}}{\beta}\ \dot{P}_2 + C_\ell\,(P_1 - P_2) \quad \ldots (3\text{-}19)$$

The orifice flow equation for this side is:

$$Q_2 = \sqrt{\frac{2}{\rho}}\ C_d\ w x_v \sqrt{P_2}$$

Considering the force equilibrium on the actuator we get:

$$M \cdot \ddot{y} = A_1 P_1 - A_2 P_2 - B_m \dot{y} + W \qquad \ldots (3\text{-}21)$$

When X_v is negative the equations for the flow Q_1 and Q_2 will change.

From figure 3-2 we see that for negative X_v

$$Q_1 = \sqrt{\frac{2}{\rho}}\ C_d\ w X_v \sqrt{P_1} \qquad \ldots.(3\text{-}22)$$

and

$$Q_2 = \sqrt{\frac{2}{\rho}}\ C_d\ w X_v \sqrt{P_s - P_2} \qquad \ldots.(3\text{-}23)$$

Equations (3-17), (3-19) and (3-21) remain the same for this case.

Note that for this case X_v, Q_1, Q_2 are negative. $\dot{y}$ can be positive for a transient condition only. y can be negative or positive depending on the starting point.

For the positive X_v case Q_1 and Q_2 are positive. $\dot{y}$ can be negative for the transient conditions only. y can be negative or positive depending on the starting point.

Combining (3-17) with (3-18), (3-19) with (3-20), (3-17) with (3-22) and (3-19) with (3-23) we get the following equations:

$$\dot{P}_1 (V_{t_1} + A_1 \cdot y) = \beta C_d \sqrt{\frac{2}{\rho}}\ w X_v \sqrt{\Delta p_1} - \beta \cdot A_1 \cdot \dot{y} - \beta C_\ell (P_1 - P_2) \qquad \ldots.(3\text{-}24)$$

$$\dot{P}_2 (V_{t_2} - A_2 \cdot y) = -\beta C_d \sqrt{\frac{2}{\rho}}\ w X_v \sqrt{\Delta P_2} + \beta \cdot A_2 \cdot \dot{y} + \beta \cdot C_\ell (P_1 - P_2) \qquad \ldots.(3\text{-}25)$$

$$\ddot{y} = \frac{A_1}{M} P_1 - \frac{A_2}{M} P_2 - \frac{B_m}{M} \dot{y} + g \qquad \ldots.(3\text{-}26)$$

$$\Delta P_1 = P_s - P_1 \quad \text{for } X_v > 0$$
$$= P_1 \quad \text{for } X_v < 0 \qquad \ldots.(3\text{-}27)$$

$$\Delta P_2 = P_2 \quad \text{for } X_v > 0$$
$$= P_s - P_2 \quad \text{for } X_v < 0 \qquad \ldots\ldots(3\text{-}28)$$

It is assumed in the above equations that ΔP_1 and ΔP_2 can never be negative, i. e. P_1 cannot exceed P_s in equation (3-18) and P_2 cannot exceed P_s in equation (3-23). This assumption is substantiated by the results from the actual system and the simulator system when it was acted upon by a large step input. However, for the case of sudden closure of the value when the load is moving initially at a considerable velocity, ΔP_1 and ΔP_2 can become negative, and equations (3-18) and (3-23) become:

$$Q_1 = \sqrt{\frac{2}{\rho}}\, C_d\, w\, X_v \sqrt{|P_s - P_1|}\ \operatorname{sgn}(P_s - P_1) \qquad \ldots\ldots(3\text{-}18a)$$

$$Q_2 = \sqrt{\frac{2}{\rho}}\, C_d\, w\, X_v \sqrt{|P_s - P_2|}\ \operatorname{sgn}(P_s - P_2) \qquad \ldots\ldots(3\text{-}23a)$$

Where $\operatorname{sgn}(P_s - P_1) = +1 \quad \text{for} \quad P_s > P_1$

$$= -1 \quad \text{for} \quad P_s < P_1$$

and $\operatorname{sgn}(P_s - P_2) = +1 \quad \text{for} \quad P_s > P_2$

$$= -1 \quad \text{for} \quad P_s < P_2$$

However, this case is not studied in this dissertation and equations (3-18a) and (3-23a) will not be considered in the development of the model.

Assuming the replenishing check valves have instantaneous response, we get:

$$P_1 \geq o \qquad \ldots.(3\text{-}29)$$

$$P_2 \geq o \qquad \ldots.(3\text{-}30)$$

(3-29) and (3-30) are valid independent of the actual values resulting from the solution of equations (3-24) through (3-28).

It is worthwhile to note at this point that the equations (3-24) through (3-30) form the basic difference between a symmetrical and asymmetrical actuator as $\Delta P_1 \neq \Delta P_2$.

The terms $(V_{t_1} + A_1 . y)$ and $(V_{t_2} - A_2 . y)$ represent the changing volumes at each chamber of the actuator as the piston extends or retracts. These terms should affect the natural frequency of the actuator which becomes a function of the position of the actuator.

An investigation was made on the analog computer to evaluate the effect on the transient responses of P_1 and P_2 to a step input of valve displacement X_v when the terms $A_1 . y$ and $A_2 . y$ were present in the chamber volumes expression and when they were removed. The response was found to be identical for the system parameters considered.

This can be explained by the fact that in the general expression for the compressibility flow $\frac{V_t \pm A.y}{\beta} \cdot \dot{P}$, $\dot{P}$ is large at the initial response of the system to the input when the system is in its rest position, i. e. when $y = 0$, while when y increases, $\dot{P}$ decays and the term has a negligible value. Hence if the system starting position is the mid stroke position, as is the case considered in this paper, the term A. y will not affect the results as confirmed by the analog computer results.

In the final system model representation these terms were removed, thus simplifying the resulting model.

Equation (3-24) and (3-25) thus become:

$$\dot{P}_1 = \frac{\beta}{V_{t_1}} C_d \sqrt{\frac{2}{\rho}} w X_v \sqrt{\Delta p_1} - \frac{\beta A_1 \cdot \dot{y}}{V_{t_1}} - \frac{C_\ell \beta (P_1 - P_2)}{V_{t_1}} \quad \ldots . (3\text{-}31)$$

$$\dot{P}_2 = -\frac{\beta}{V_{t_2}} C_d \sqrt{\frac{2}{\rho}} w X_v \sqrt{\Delta p_2} + \frac{\beta A_2 \cdot \dot{y}}{V_{t_2}} + \frac{\beta C_\ell}{V_{t_2}} (P_1 - P_2) \quad \ldots . (3\text{-}32)$$

3. 2. 1. 4 Summing Junction Model

The error voltage from the summer is:

$$E_i = V_i - V_f \quad \ldots . (3\text{-}33)$$

and $V_f = G_f \cdot y \quad \ldots . (3\text{-}34)$

The RC network output is:

$$E_o(s) = \frac{E_i(s)}{S + \frac{1}{RC}}$$

or

$$\dot{E}_o = E_i - \frac{1}{RC} \cdot E_o \qquad \ldots\ (3\text{-}35)$$

Combining equations (3-33), (3-34) and (3-35) we get:

$$\dot{E}_o = (V_i - G_f \cdot y) - \frac{1}{RC} E_o \qquad \ldots\ (3\text{-}36)$$

The input current to the valve is:

$$I_s = \frac{10^3 . Eo}{R_v} \times G_a \qquad \ldots\ (3\text{-}37)$$

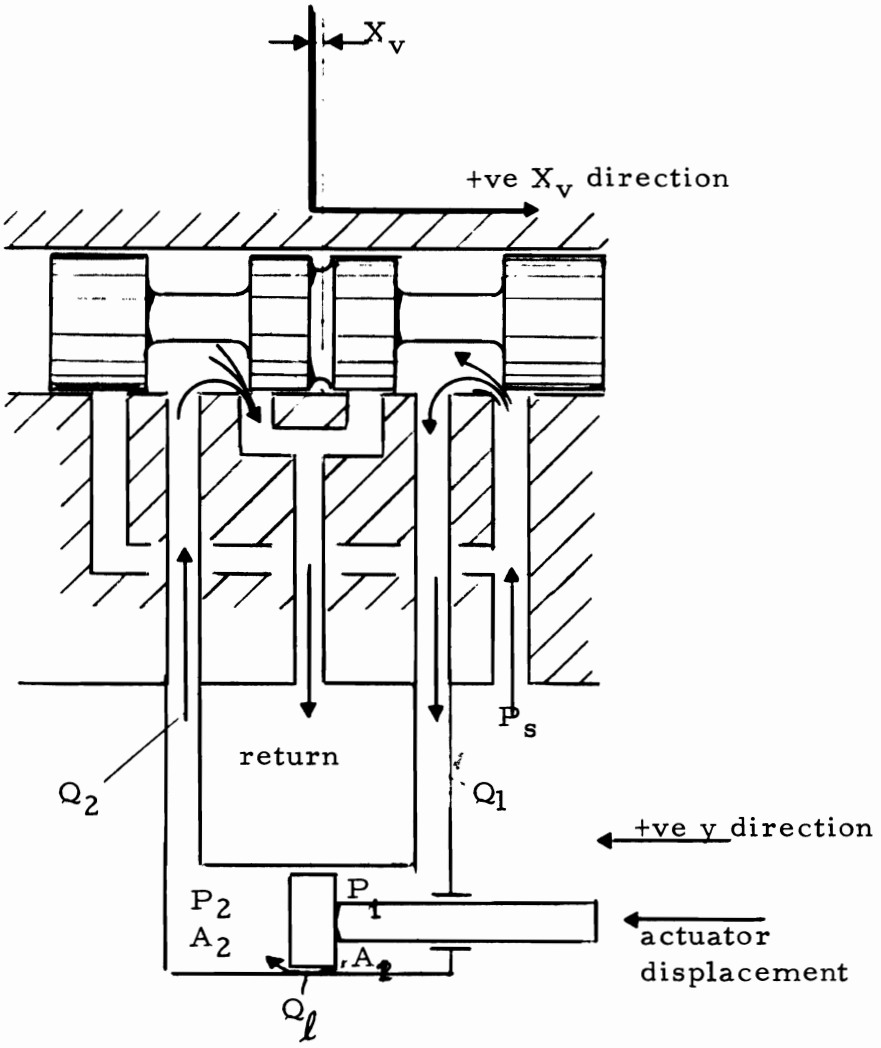

Figure 3-1 Flow Configuration for Positive Spool Displacement

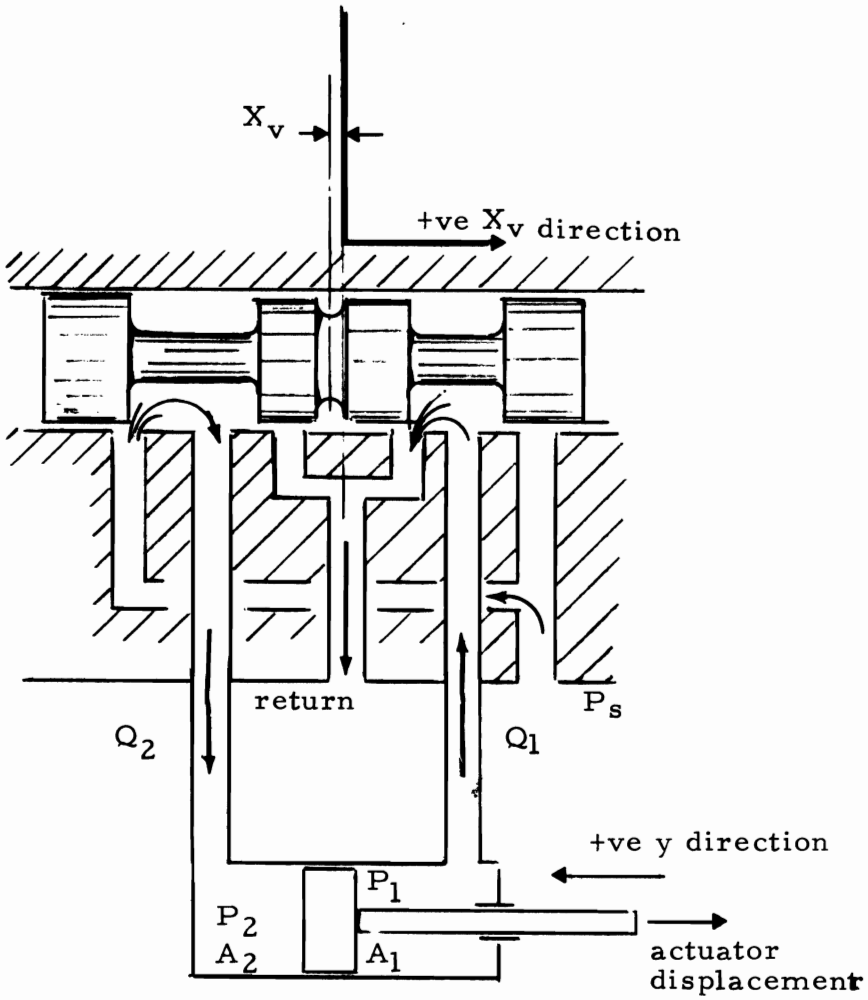

Figure 3-2 Flow Configuration for Negative Spool Displacement

Chapter 4

SIMULATION & INTERPRETATION OF RESULTS

4.1 Introduction

The system equations developed in Chapter 3 describing the considered physical system and forming its mathematical model were solved on an EAI 680 analog computer.

The analog computer is especially suitable for the simulation of the system considered rather than a digital computer. A similar hydraulic system was simulated by ODIERNA (23) on an IBM 360/50 using FORTRAN IV computer program in double precision requiring 100k bytes. Using a quadrature interval of 50 micro-seconds 3.5 hours of computer time was used for 1.4 seconds of real time.

The reason for the very small quadrature intervals can be attributed to the high value of the effective oil bulk modules which resulted in very large values for the rate of change of pressure.

On the other hand the accuracy of the analog computer is adequate enough for the practical use of the simulation, though, of course there is the amplitude and time scaling requirements to

to take into account when using the analog computer.

In the next sections the simulation procedure is detailed and the responses of some of the system variables are shown. Recordings of the response of the physical system variables were obtained during its test and compared to the corresponding results from the simulation.

4.2 Simulation

In order to arrive at a reasonably accurate model without including those parameters which have negligible effect on the results the simulation was done in steps.

The first step was to evaluate the effect of including the spool flow forces. This was done on a model with symmetrical loading (hydraulic motor) as presented in (12). A detailed discussion is found in Appendix "A" and equation (3-15) describes the final model.

Concluding from the results that the spool flow forces have negligible effect on the results, these were excluded from the final model.

Next, the effect of varying oil volume was studied on a model

that simulated the second stage of the valve and the linear actuator with differential areas.

The response of P1 and P2 were compared for a step spool movement with and without the changing volume terms. The results were practically identical as explained in section 3.2.2.

Hence these terms were not included in final model.

The final model is represented by the equations developed in chapter 3 and summarized below:

$$\ddot{x}_f = -2\omega_n \zeta_n \dot{x}_f - \omega_n^2 x_f + K_1 \omega_n^2 x_v \quad \ldots\ldots (3\text{-}7)$$

$$\dddot{x}_v = \frac{K_2}{A_v} \omega_h^2 x_f - 2\delta_h \omega_h \ddot{x}_v - \omega_h^2 \dot{x}_v \quad \ldots\ldots (3\text{-}16)$$

$$\ddot{y} = \frac{A_1}{M} P_1 - \frac{A_2}{M} P_2 - \frac{B_m}{M} \dot{y} + g \quad \ldots\ldots (3\text{-}26)$$

$$\Delta p_1 = P_s - P_1 \quad \text{for} \quad x_v > 0$$
$$= P_1 \quad \text{for} \quad x_v < 0 \quad \ldots\ldots (3\text{-}27)$$

$$\Delta p_2 = P_2 \quad \text{for} \quad x_v > 0 \quad \ldots\ldots (3\text{-}28$$
$$= P_s - P_2 \quad \text{for} \quad x_v < 0$$

$$P_1 \geq 0 \qquad \ldots\ (3\text{-}29)$$

$$P_2 \geq 0 \qquad \ldots\ (3\text{-}30)$$

$$\dot{P}_1 = \frac{\beta}{V_{t_1}} C_d \sqrt{\frac{2}{\rho}}\ w\, x_v \sqrt{\Delta P_1} - \frac{\beta A_1}{V_{t_1}} \dot{y} - \frac{\beta . C_\ell}{V_{t_1}} (P_1 - P_2) \qquad \ldots\ (3\text{-}31)$$

$$\dot{P}_2 = -\frac{\beta}{V_{t_2}} C_d \sqrt{\frac{2}{\rho}}\ w\, x_v \sqrt{\Delta P_2} + \frac{\beta A_2}{V_{t_2}} \dot{y} + \frac{\beta C_\ell}{V_{t_2}} (P_1 - P_2) \qquad \ldots\ (3\text{-}32)$$

$$\dot{E}_0 = (V_i - G_f \cdot y) - \frac{1}{RC} E_0 \qquad \ldots\ (3\text{-}36)$$

$$I_s = 10^3 \frac{E0}{R_v} \cdot G_a \qquad \ldots\ (3\text{-}37)$$

The scaling of the equations, the determination of the coefficients and the analog patching diagram are shown in Appendix 'D'.

The numerical values of the parameters are given in Appendix "C" while the symbols are defined in Appendix "E" as mentioned earlier.

Studying the parameters of the system components it becomes apparent that the servo valve dynamics are much faster than those of the actuator. This results in the need for slowing down the computer time by a factor of 1000 and in very low values for the pots preceding the actuator velocity and displacement integrators. This is also reflected by the requirement to attenuate the error voltage (and hence the current) variation rate feeding into the valve in the actual system. The first stage natural frequency, for example, defined in section 3-2-1-1 as $\omega_n = \sqrt{\frac{K_f}{J_f}}$ is 4580 rad./sec or 730 cps. For comparison, the hydraulic natural frequency for the actuator as given by (22) is:

$$\omega_a = \left[\frac{\beta A_2^2}{M} \left(\frac{1}{V_{t_1}} + \frac{1}{V_{t_2}} \right) \right]^{1/2} = 74.5 \text{ rad./sec. or}$$

11.85 cps.

4.3 Simulation Results

The variables of particular interest in this study are the actuator displacement, the actuator velocity and the pressures in the two actuator chambers. The variables recorded from the physical system are the actuator displacement and velocity, and the actuator full end chamber pressure. The valve spool displacement is significant in determining the effect the servo valve performance has on the whole system.

The most significant system behaviour is for step voltage inputs and this will form the basic type of input command for the purpose of this study.

The supply pressure is maintained at 1500 psi throughout the simulation, the same as in the physical system.

4. 3. 1 Spool Displacement

Figure 4-1 shows the valve spool displacement compared with the error voltage E_o at the output of the RC network, which is propositional to the input current to the valve for a command step input. The displacement follows the current with a lag of . 020 secs. Thereafter the spool displacement curves will provide the basis for studying the other variables performance.

4. 3. 2 Actuator Velocity

Figures 4-2 through 4-5 show the actuator velocity compared with the spool displacement response to a step input. The velocity curve follows the spool displacement curve with an initial lag of . 020 secs.

In comparing Figure 4-2 with 4-3 it is found that the time required for the first cycle of the spool displacement, i. e. from the starting point to the first spool reversal, is greater

when the actuator extends (negative command) than when it retracts (positive command), due to the weight bias. The same applies to the next cycle, i. e. retracting, except that in this case the spool displacement is negative for the positive command and vice versa.

Also the maximum velocity achieved in extension is lower than that achieved in retraction, the ratio being 1:1. 35, though the spool opening is approximately 5% larger in extension.

The velocity response is more damped in extension (against the weight) than in retraction. Also the velocity response is more damped for larger step inputs than for small step inputs as could be observed by comparing Figures 4-2 and 4-3 with Figures 4-4 and 4-5 respectively.

4. 3. 3 Actuator Displacement

Figures 4-6 and 4-7 show the actuator displacement compared to the valve spool displacement for a step input response. Figures 4-8 and 4-9 show the actuator displacement response to other step inputs.

The actuator displacement response has an initial lag of .050 secs. behind the spool displacement response.

The spool displacement reaches its maximum value after a constant time value for all positive step inputs and after a different but constant value for all negative step inputs.

The same applies for the actuator displacement.

Although the ratio of maximum values of spool displacement is not proportional to the ratio of the input step sizes, the ratios of maximum actuator displacements are:

Also the ratio of the maximum actuator displacement to its steady state value is constant for all step inputs shown, being 1.16 in retraction and 1.085 in extension.

Consequently, the steady state values of actuator displacement are linearly proportional to the input step for each case; extension and retraction.

The steady state values of actuator displacement in retraction are 4% higher than for extension.

4.3.4 Pressure Response

Figures 4-10 and 4-11 show the response of the full end and rod end chamber pressures to a positive step input (actuator

retracting). The full end chamber pressure P_2 has an initial value of $\frac{W}{A_2}$ to balance the weight. As the spool moves to connect this chamber to the return line it causes a drop in the pressure value, but with increasing absolute value of the velocity the pressure drop Δp_2 and consequently P_2, which in this case equals Δp_2, increase.

From equation (3-32), neglecting $\dot{P}_2$ which tends to zero after the initial response period, and neglecting the leakage flow as being negligible, we get:

$$\Delta p_2 = \left(\frac{A_2 \dot{y}}{C_d \sqrt{\frac{2}{\rho}} \, w \cdot x_v} \right)^2$$

As $\dot{y}$ tends to follow x_v as shown in section 4. 3. 2 the ratio $\dot{y}/x_v$ tends to be almost constant as both values tend to zero. Therefore, P_2 tends to be almost constant up to the spool reversal. At this moment the full end chamber is connected to the system pressure and the actuator is extending. The pressure at this period (negative x_v) according to equation (3-28) will be:

$$P_2 = P_s - \Delta p_2$$

and as the extension velocity and consequently Δp_2 increase, P_2 drops and eventually stabilizes at its steady state value at a slow rate when $\dot{y}$ approaches zero. The rod end chamber pressure P_1 tends to reach the supply pressure value as the spool moves to

connect this chamber to the supply pressure.

Equation (3-27) states:

$$P_1 = P_s - \Delta p_1$$

The increasing actuator velocity causes a higher pressure drop across the spool, Δp_1, and P_1 oscillates around a value which is lower than the supply pressure. The fact that P_1 does not vary significantly up to the spool reversal can be explained by the same reasoning applied to P_2 for this period.

After the spool reversal the rod end chamber is connected to the return line and the pressure drops and eventually reaches its steady state value at a slow rate.

Figures 4-12 and 4-13 show the response of P_2 and P_1 to a negative step input of the same magnitude. No significant change is observed in P_2 while P_1 increases considerably as the spool reversal causes the rod end chamber to be connected to the supply pressure.

It is worthwhile to note that the pressures P_1 and P_2 did not exceed the supply pressure and the assumption made in section 3.2.2 is justified.

The steady state values of P_1, P_2 and x_v can be calculated as follows:

The same leakage flow passes through the two spool orifices. These orifices being of the same area due to symmetry we get:

$$\Delta p_1 = \Delta p_2 \qquad \ldots\ (4\text{-}1)$$

but

$$\Delta p_1 = P_1 \qquad \ldots\ (4\text{-}2)$$

and

$$\Delta p_2 = P_s - P_2 \qquad \ldots\ (4\text{-}3)$$

From the force equilibrium we get:

$$A_2 P_2 - A_1 P_1 = W \qquad \ldots\ (4\text{-}4)$$

The values of the variables in these equations are their steady state values.

Combining (4-1), (4-2) and (4-3) we get:

$$P_2 + P_1 = P_s \qquad \ldots\ (4\text{-}5)$$

Solving (4-4) and (4-5) we obtain the steady state values of P_1 and P_2:

$$P_2 = \frac{W + A_1 P_s}{A_1 + A_2} \qquad \ldots\ (4\text{-}6)$$

$$P_1 = P_s - \frac{W + A_1 P_s}{A_1 + A_2} \qquad \ldots\ (4\text{-}7)$$

Inserting the values of W, A_1, A_2 and P_s from Appendix "C" we get:

$$P_2 = 984 \text{ psi}$$

$$P_1 = 516 \text{ psi}$$

To obtain the steady state value of x_v, we have:

$$Q_\ell = -C_\ell (P_2 - P_1) = C_d w \sqrt{\frac{2}{\rho}} \; x_v \sqrt{\Delta p_1} \qquad \ldots . \; (4\text{-}8)$$

Combining (4-2) and (4-8) we get:

$$x_v = - \frac{C_\ell (P_2 - P_1)}{C_d w \sqrt{\frac{2}{\rho}} \; P_1} \qquad \ldots . \; (4\text{-}9)$$

Inserting the values of P_2 and P_1 as obtained above and the values of C_ℓ and $C_d w \sqrt{\frac{2}{\rho}}$ from Appendix "C" we get:

$$X_v = -.0000507 \text{ in.}$$

Figures 4-14 and 4-15 show the Δp_2 and Δp_1 responses for a positive step input while Figures 4-16 and 4-17 show the Δp_2 and Δp_1 responses for a negative step input. The effect of the spool reversals is clearly indicated as determined by equations (3-27) and 3-28).

For the portion when x_v is positive, Δp_2 in Figures 4-14 and 4-16 is identical with P2 in the same portions of Figures 4-10 and 4-12 respectively.

For the portion when x_v is negative, Δp_l in Figures 4-15 and 4-17 is identical with the same portions of Figures 4-11 and 4-13 respectively.

4.4 Actual Results

Recordings from the test of the physical system are shown in Figures 4-18 through 4-21 showing the response of the actuator velocity and displacement, the error voltage and the full end pressure to two different size step inputs both in retraction and extension.

The error voltage in this case is the input to the valve and servos as an indication of the spool displacement as Figure 4-1 shows proportionality between the spool displacement and the error voltage for step inputs.

The velocity was measured as an output voltage from a SERVO TEK SU780D-1 tachogenerator with 45 VDC per 1000 RPM.

The position was measured as an output voltage from a BOURNS Model 3451, 10 turn rotary potentiometer.

The pressure was measured as an output voltage from a SPARTON pressure transducer calibrated at 1250 psi per volt, with a range

of 0 to 10,000 psi. The tests were conducted with the mid stroke position as the starting point and with all six servo actuator assemblies moving simultaneously so that the weight distribution change was minimal during the extension and retraction of the measured actuator.

The results are comparable to those shown in section 4.3 in trend and in settling time but differ in value. Some of the common characteristics of the results are:

(1) The ratio of the maximum retraction velocity to the maximum extension velocity for the same value of the step input is the same, i.e. 1:1.35.

(2) The extension period is longer than the retraction period as explained in section 4.3.2.

(3) The time elapsed to achieve maximum velocity in extension is the same for different size step inputs. The same applies for retraction.

(4) The velocity response is more damped for larger size step inputs.

(5) The full end pressure response shows the effects of spool reversals exactly as predicted by the simulation.

(6) The steady state actuator displacement shows accurate correspondence between the simulated and actual valves.

The following deviations between the simulation and actual test results are observed:

(1) The maximum error voltage is larger in the actual system than in the simulation results for the same step input.

(2) The maximum velocity achieved for a certain maximum error voltage is lower in the actual system than in the simulated results. This ratio is lower in extension than in retraction for both the actual system and the simulation results. However, in the actual system the ratio increased with the size of the step input, from 2. 40 in. /sec. /volt for . 5 volt step input to 3. 90 in. /sec/volt for 2. 0 volts step input, in retraction and from 1. 66 in. /sec/volt for . 5 volt step input to 2. 95 in. /sec/volt for 2. 0 volts step input, in extension.

In the simulated results an average of 4. 8 in. /sec/volt was achieved in retraction and 3.4 in./sec/volt in extension.

It is worthwhile to note that the ratios:

$$\frac{2.4}{1.66} \approx \frac{3.90}{2.95} \approx \frac{4.8}{3.4} \approx 1.35$$

which is the ratio of the maximum retraction velocity to the maximum extension velocity.

(3) An inflexion point is observed in the actual velocity response as the velocity tends to reverse after reaching its maximum value. This can be due to an electronic circuit which reduces the amplifier gain G_a at a low error voltages which was taken into account in the mathematical model. Also, valve spool overlap can produce a similar effect.

As discussed above, the results indicate deviations in the velocity responses but better correspondence in the actuator displacement and pressure responses.

The analog simulation proved to be a valuable method for solving the mathematical model. Also the results helped in determining some of the correlations between the mathematical model and the physical system.

In the next chapter a summarizing discussion of the results will be given.

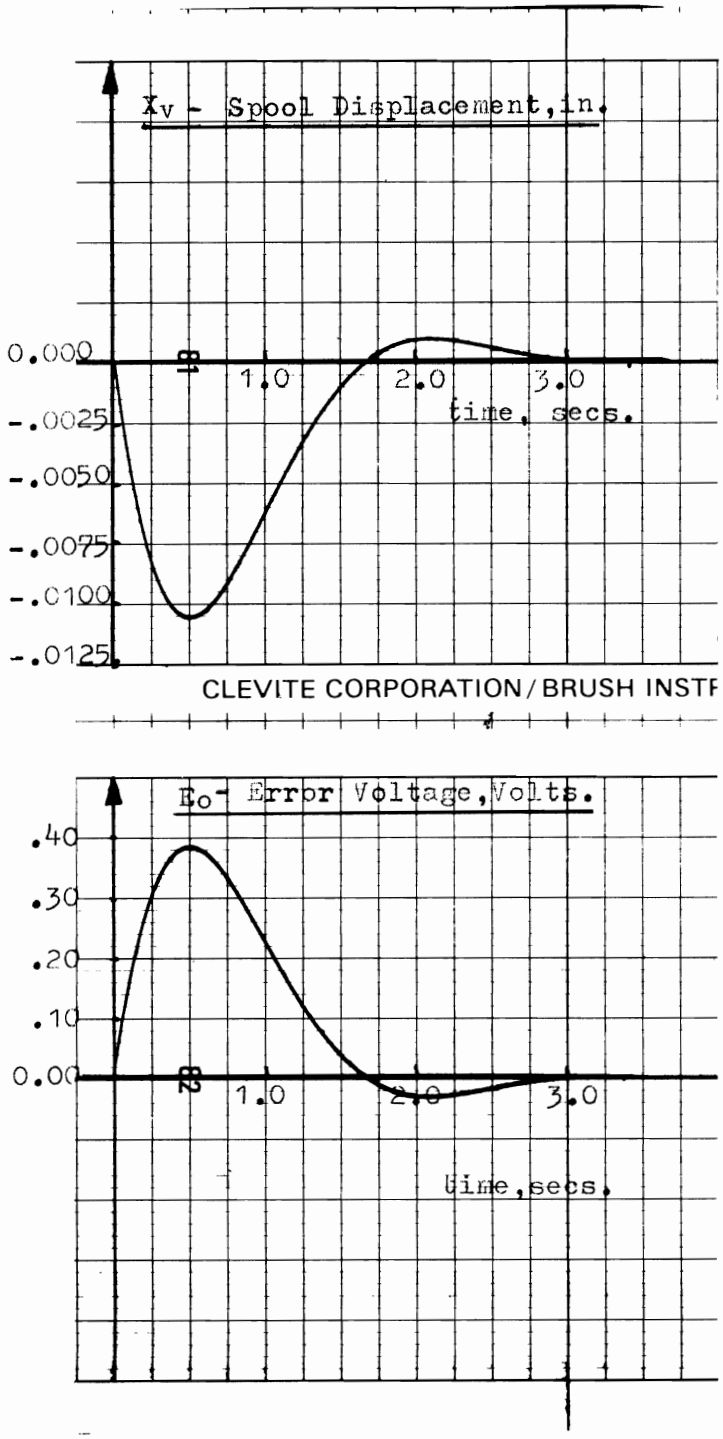

Figure 4-1 System Response to a Step Input of -2.0 Volts

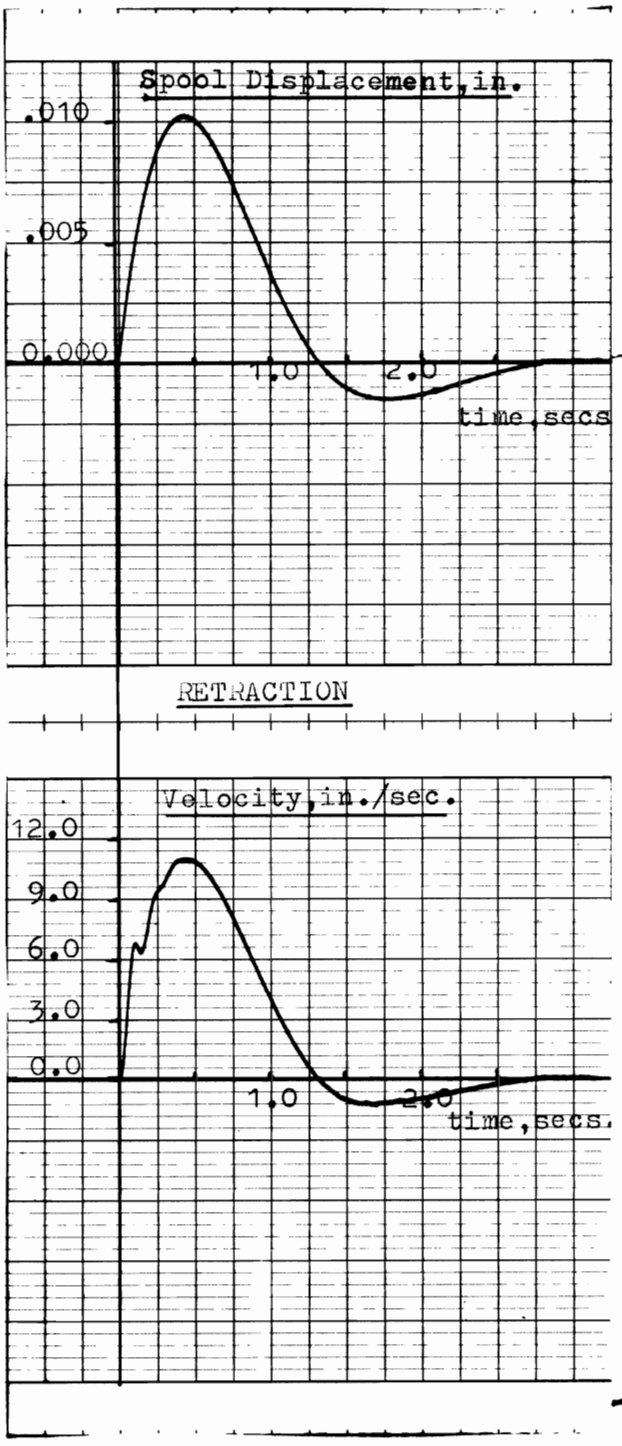

Figure 4-2 System Response to a Step Input of +2. 0 Volts

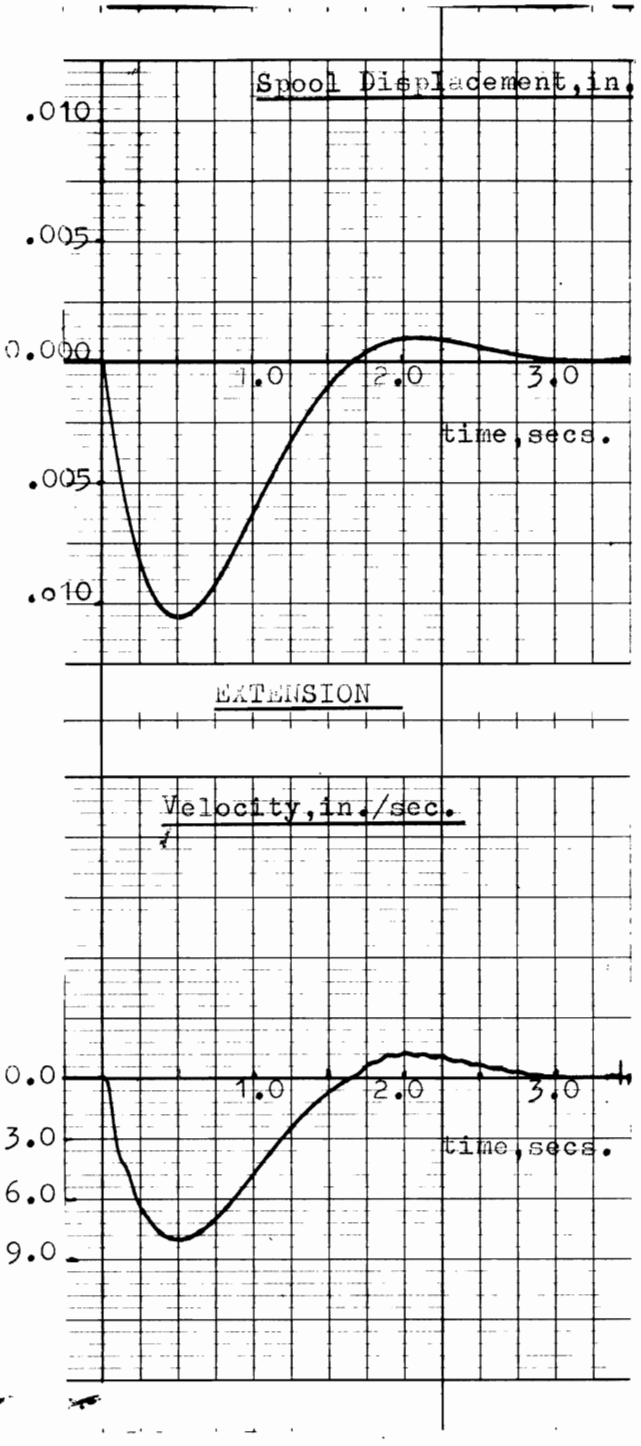

Figure 4-3 System Response to a Step Input of -2. 0 Volts

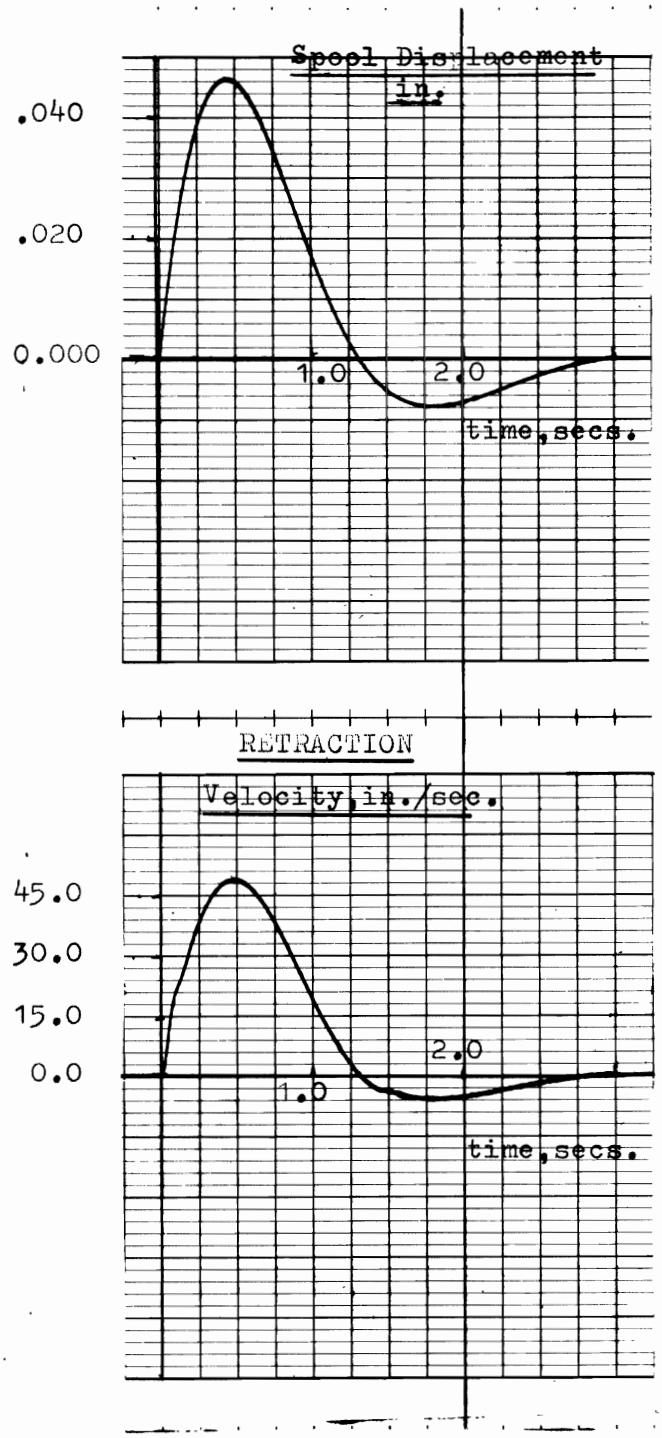

Figure 4-4 System Response to a Step Input of +9.0 Volts

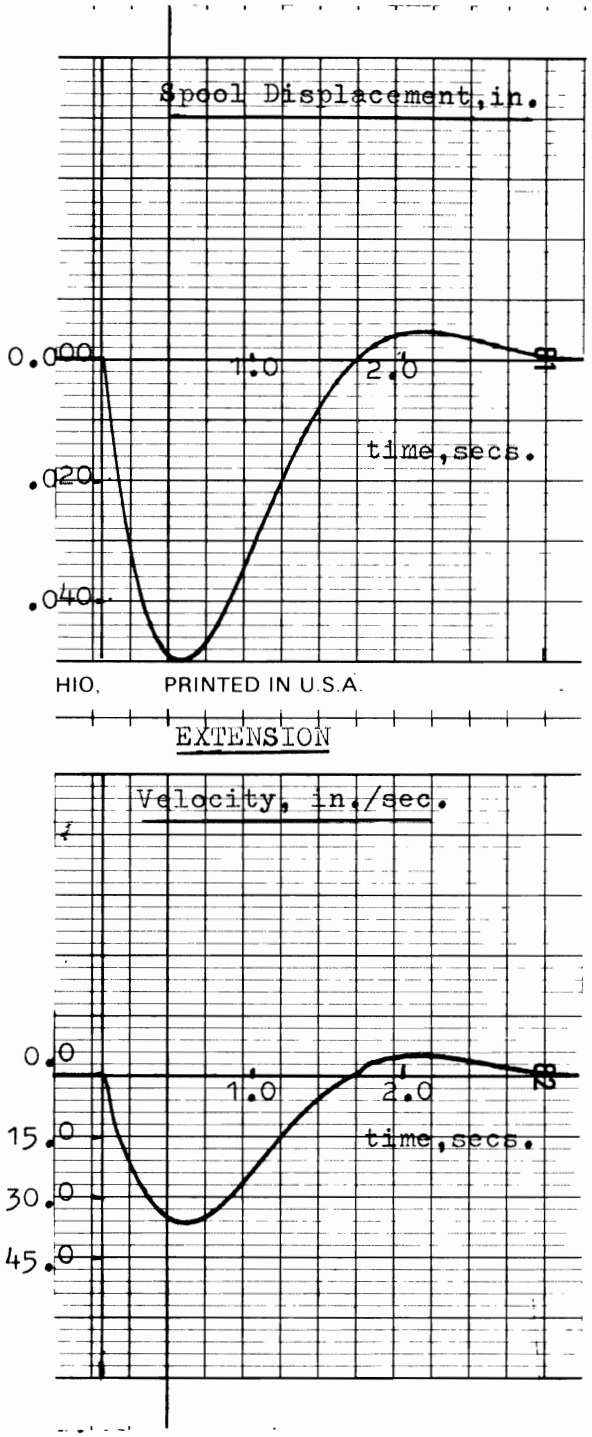

Figure 4-5 System Response to a Step Input of -9.0 Volts

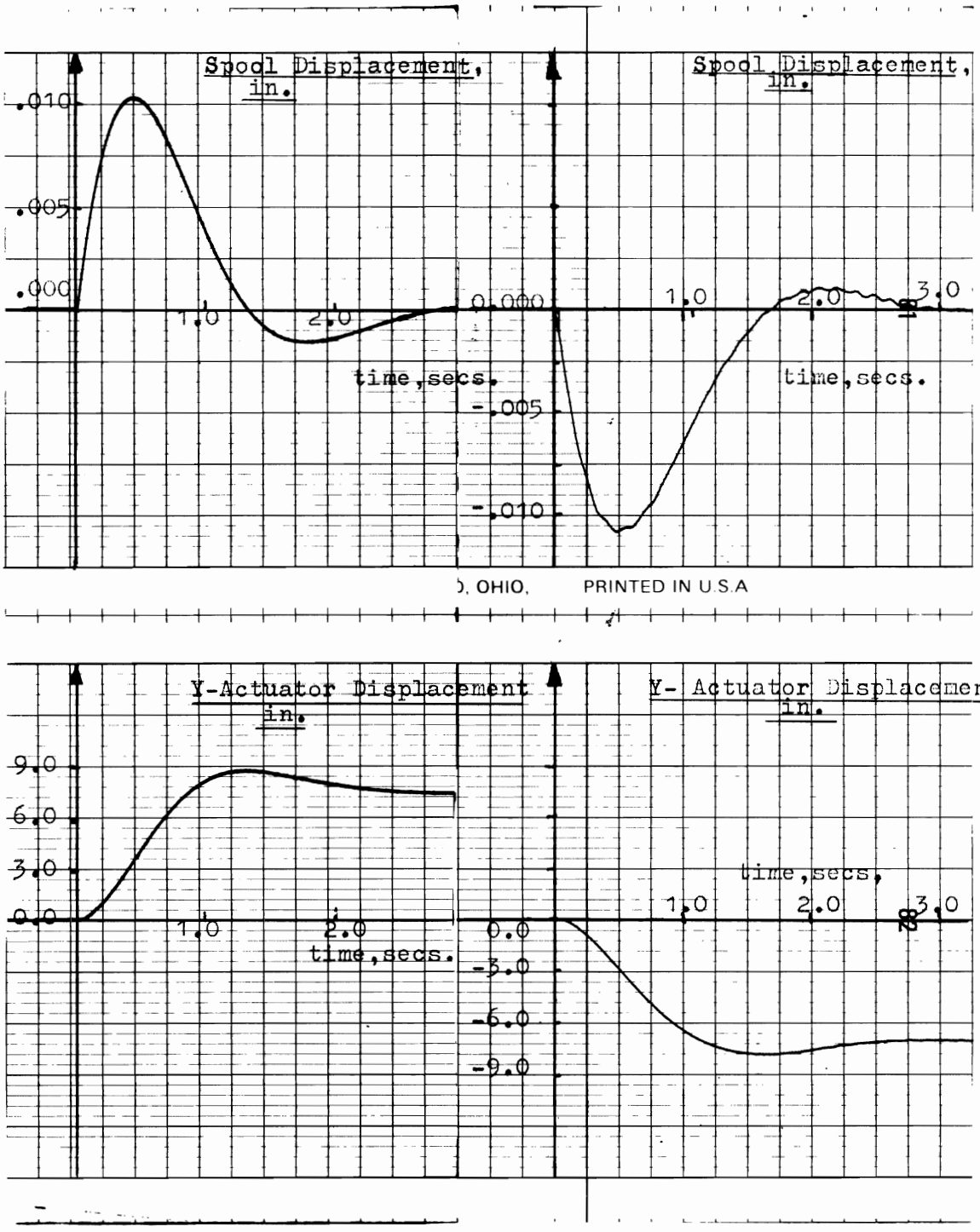

Figure 4-6 Actuator Displacement Response to a Step Input of +2.0 Volts

Figure 4-7 Actuator Displacement Response to a Step Input of -2.0 Volts

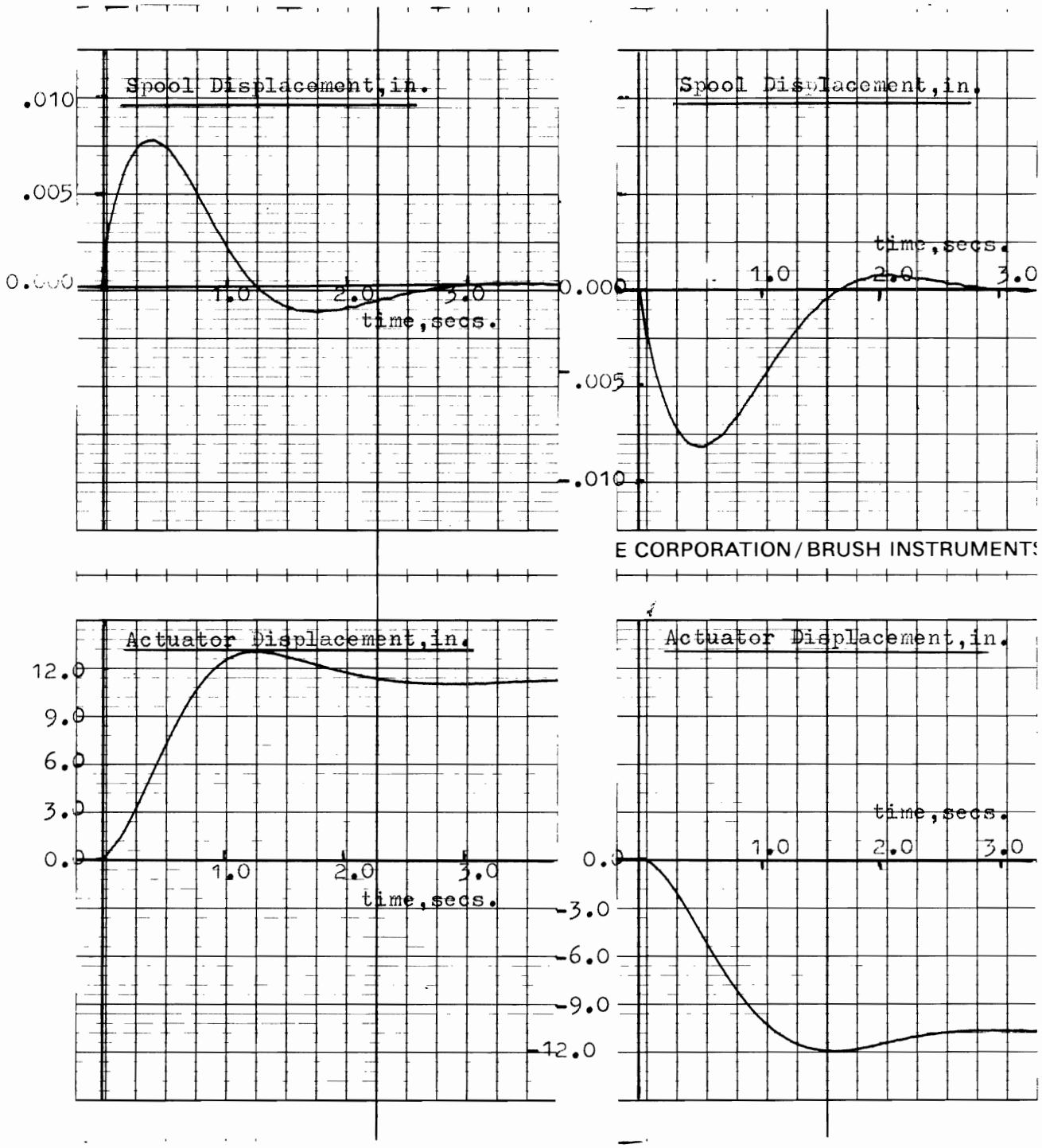

Figure 4-8 Actuator Displacement Response to a Step Input of +3.0 Volts

Figure 4-9 Actuator Displacement Response to a Step Input of -3.0 Volts

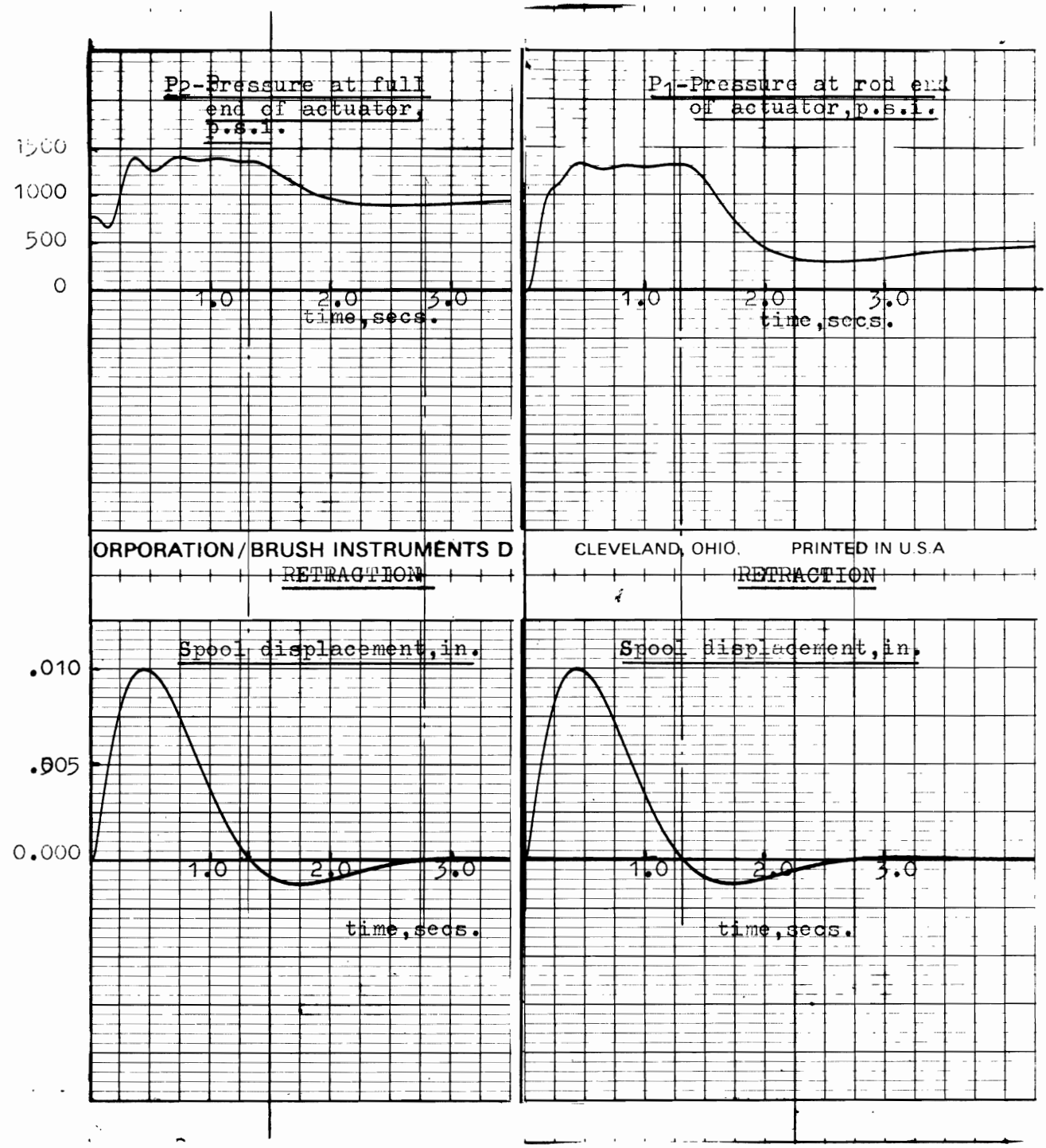

Figure 4-10 Full End Pressure Response to a Step Input of +2. 0 Volts

Figure 4-11 Rod End Pressure Response to a Step Input of +2. 0 Volts

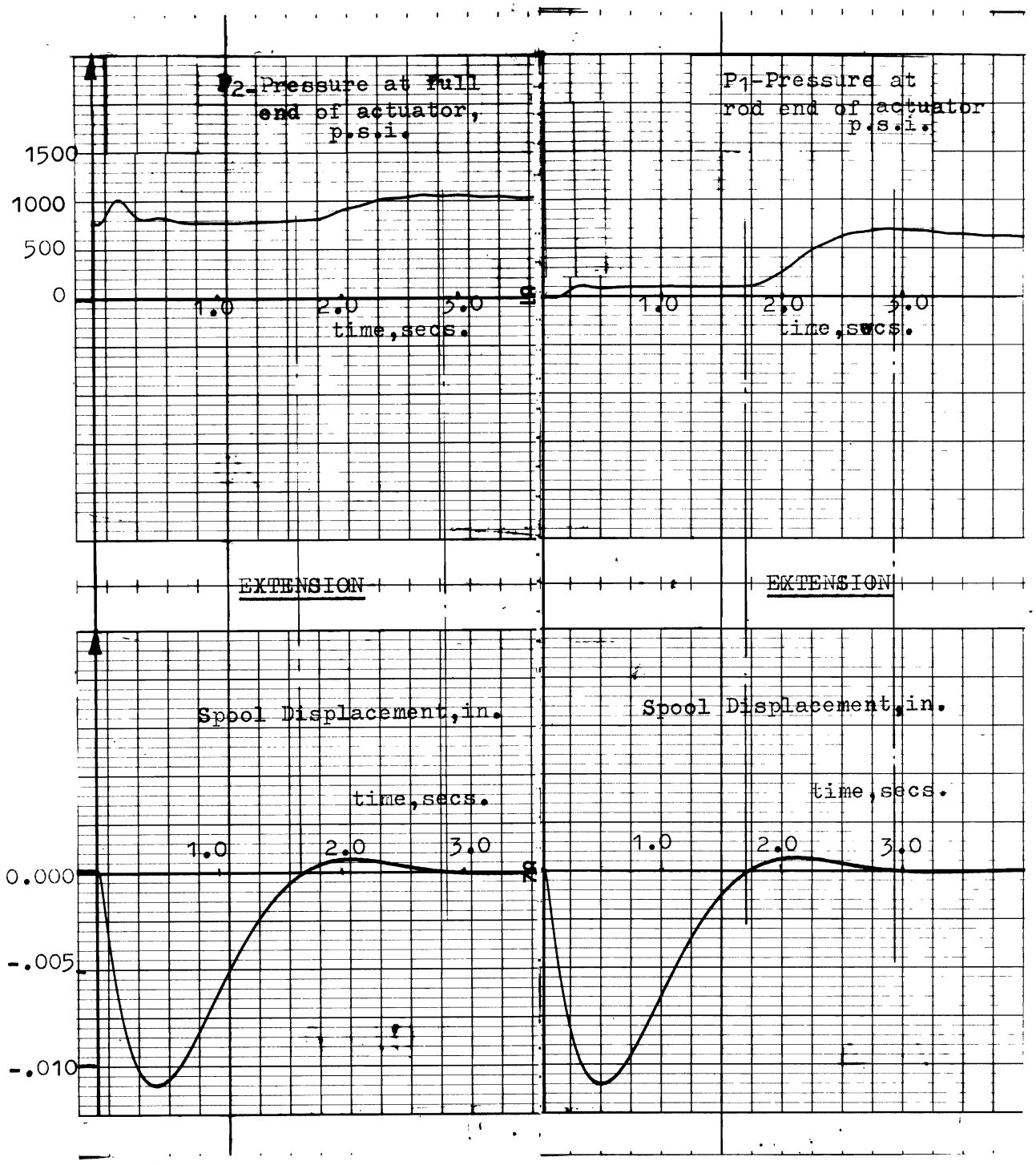

Figure 4-12 Full End Pressure Response to a Step Input of -2.0 Volts

Figure 4-13 Rod End Pressure Response to a Step Input of -2.0 Volts

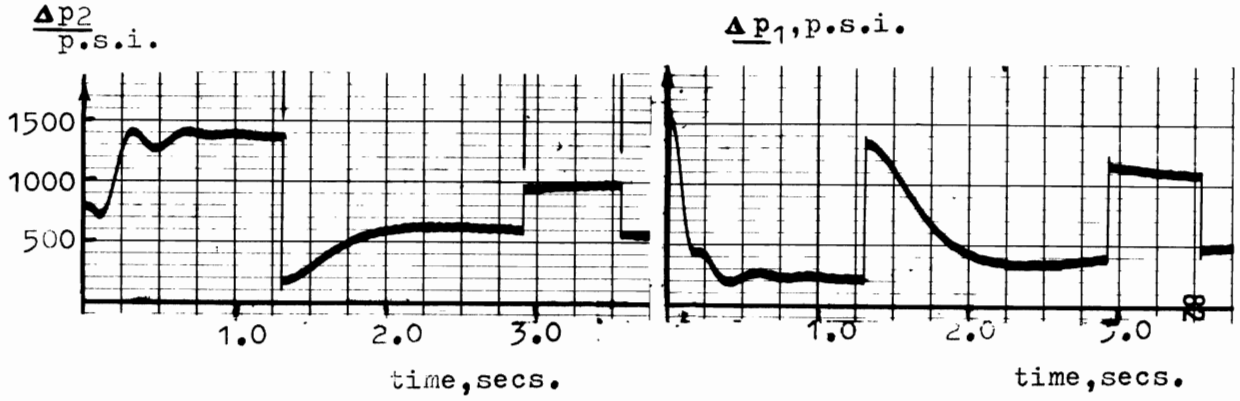

Figure 4-14 Response of ΔP_2 to a Step Input of +2.0 Volts

Figure 4-15 Response of ΔP_1 to a Step Input of +2.0 Volts

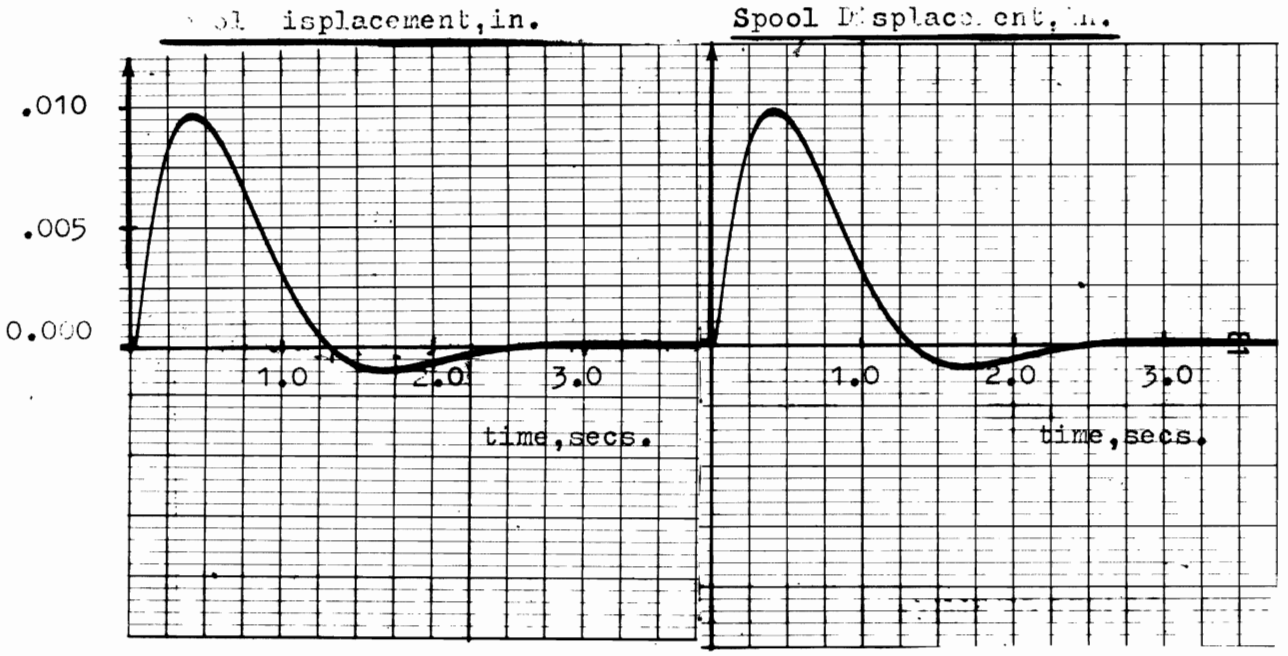

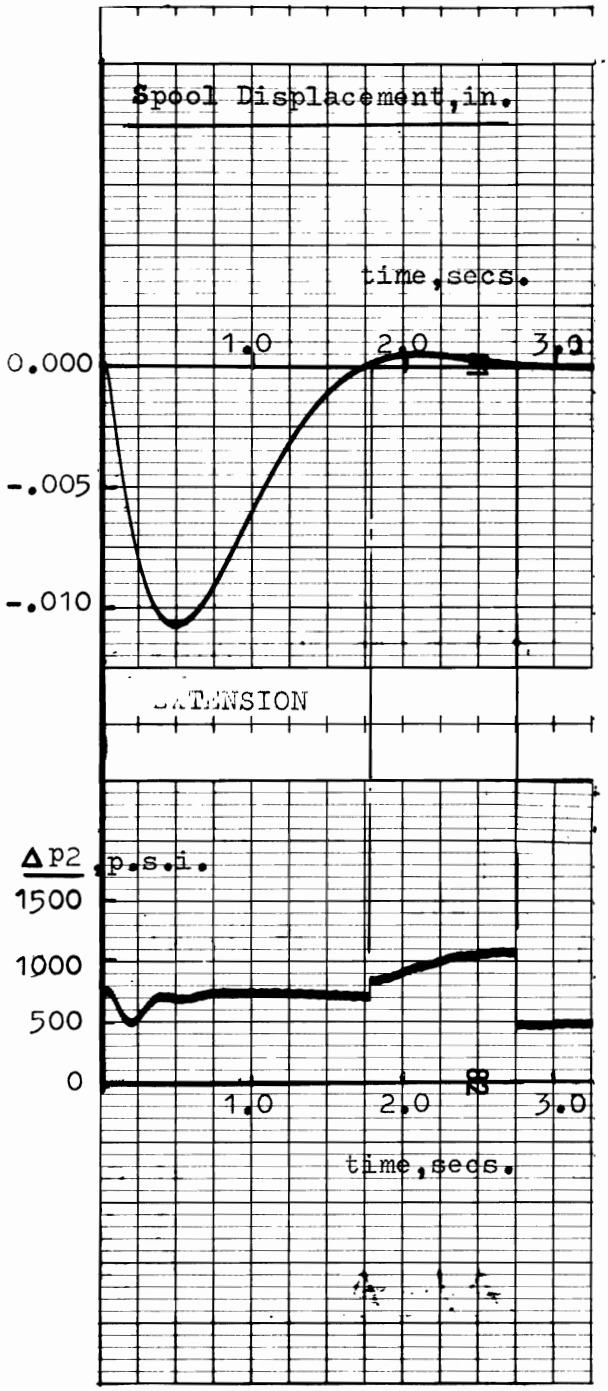

Figure 4-16 Response of ΔP_2 to a Step Input of -2.0 Volts

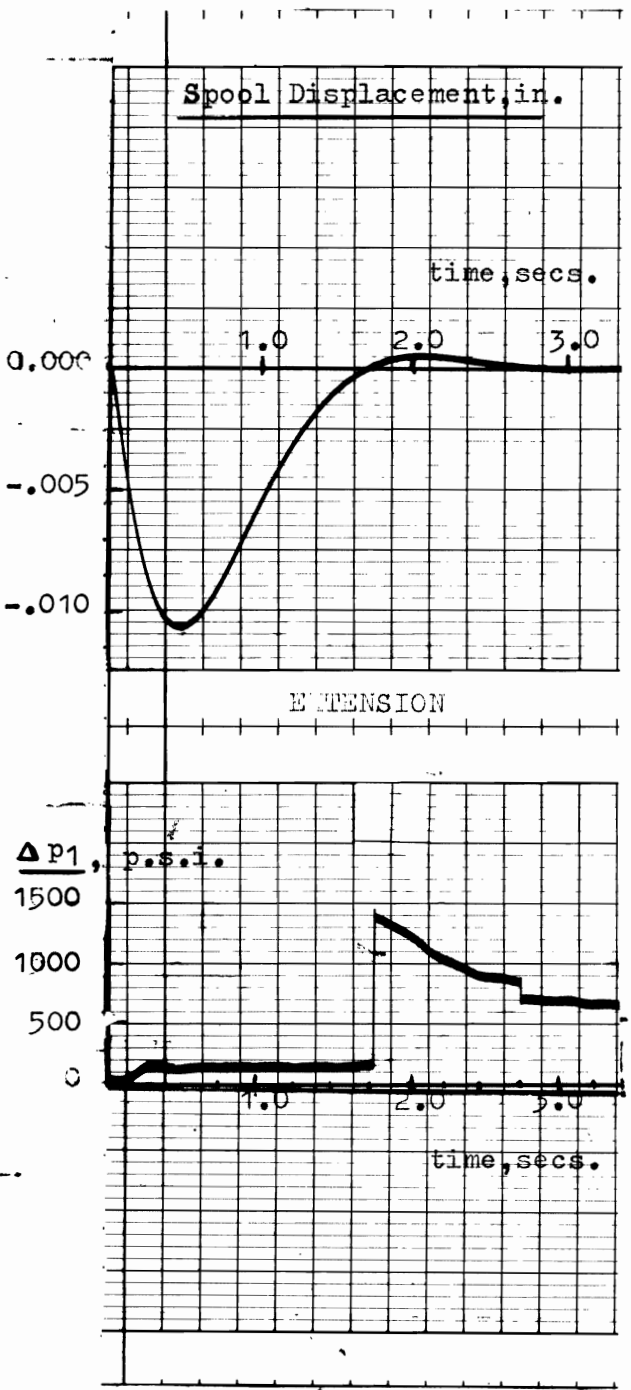

Figure 4-17 Response of ΔP_1 to a Step Input of -2.0 Volts

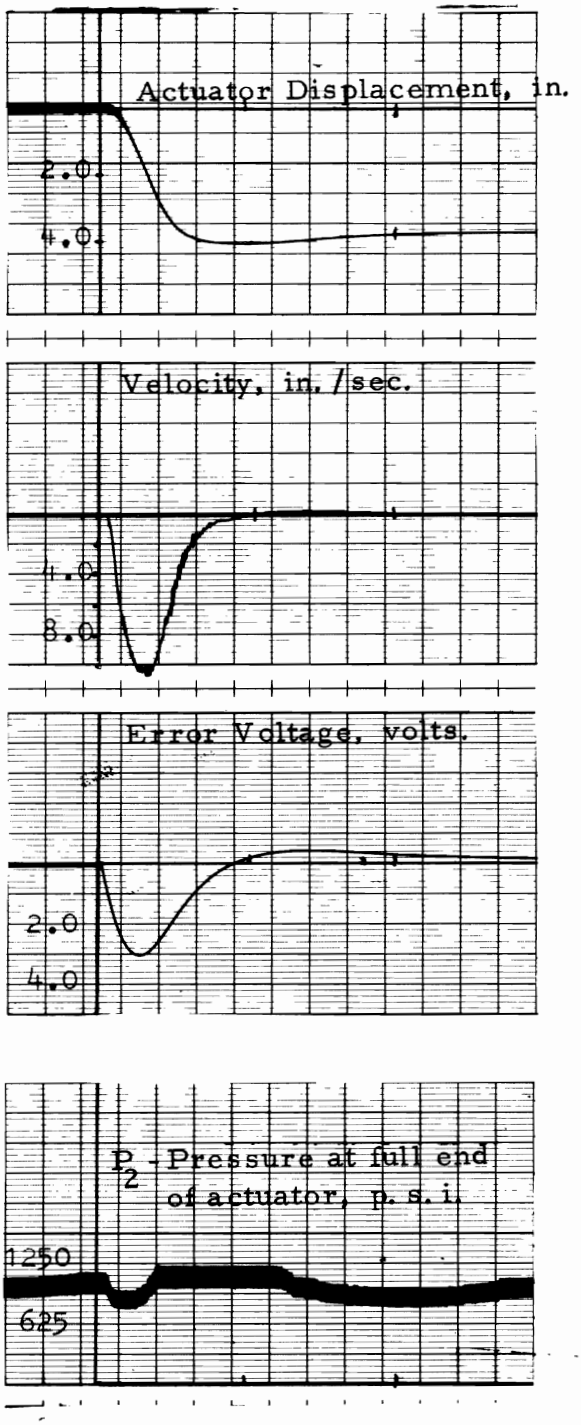

Figure 4-18 Actual System Performance for a Step Input of 1.0 Volt - Retraction

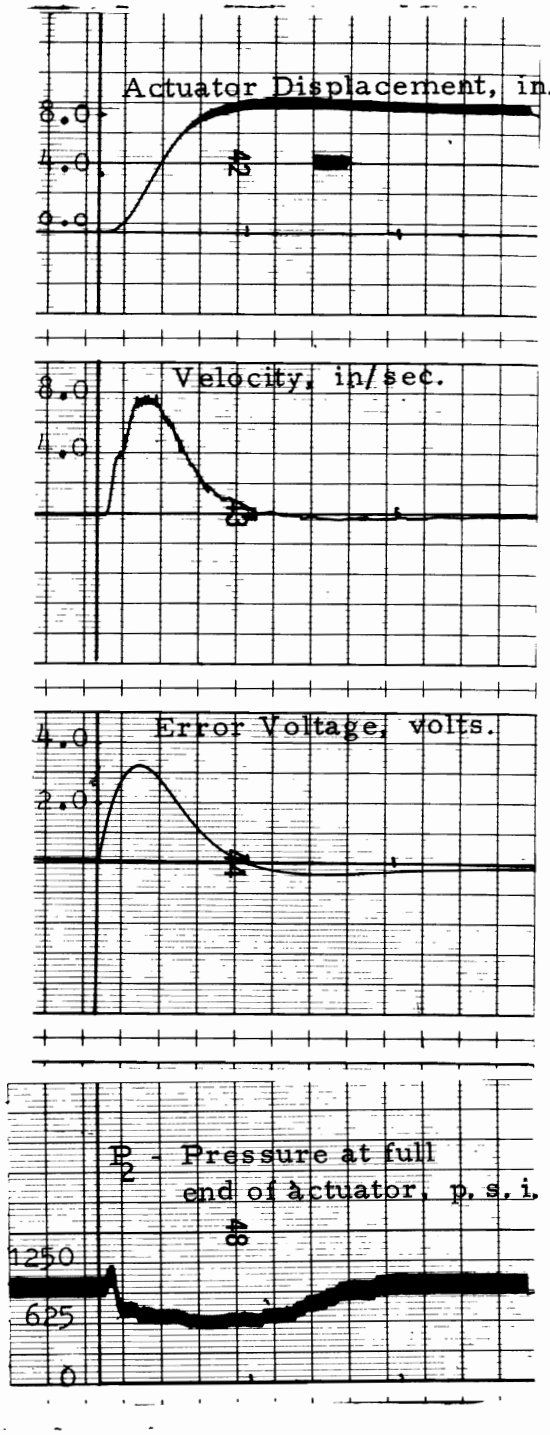

Figure 4-19 Actual System Performance for a Step Input of 1.0 Volt - Extension

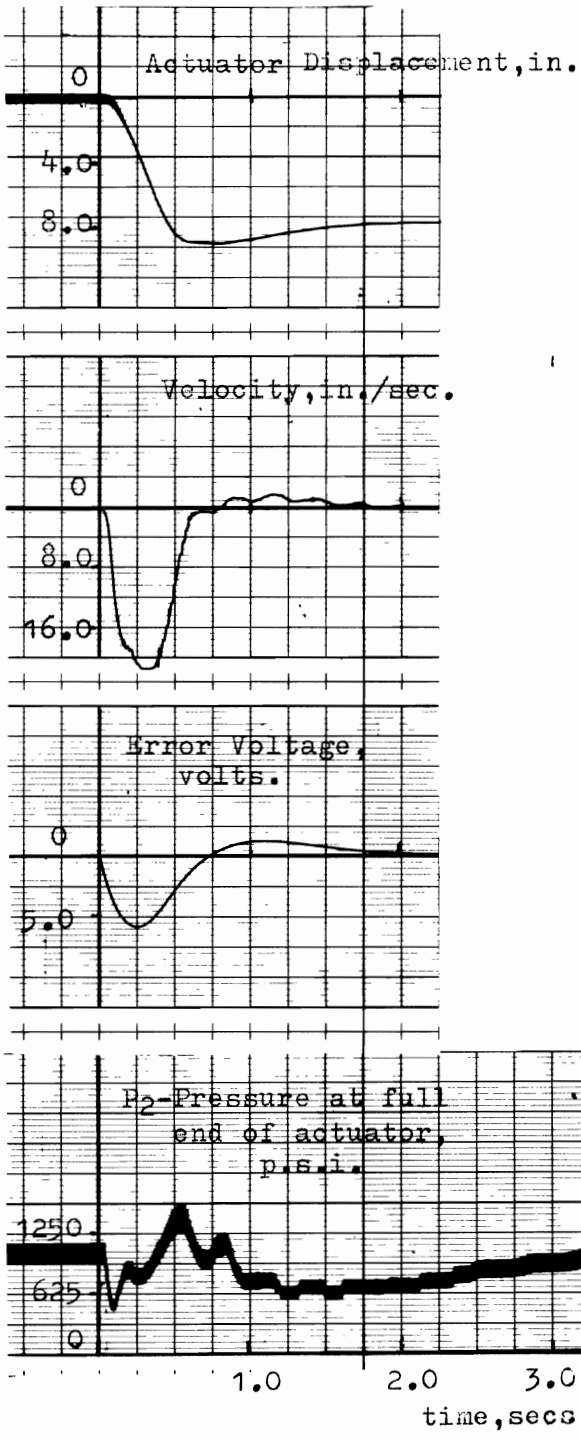

Figure 2-20 Actual System Performance for a Step Input of 2. 0 Volts - Retraction

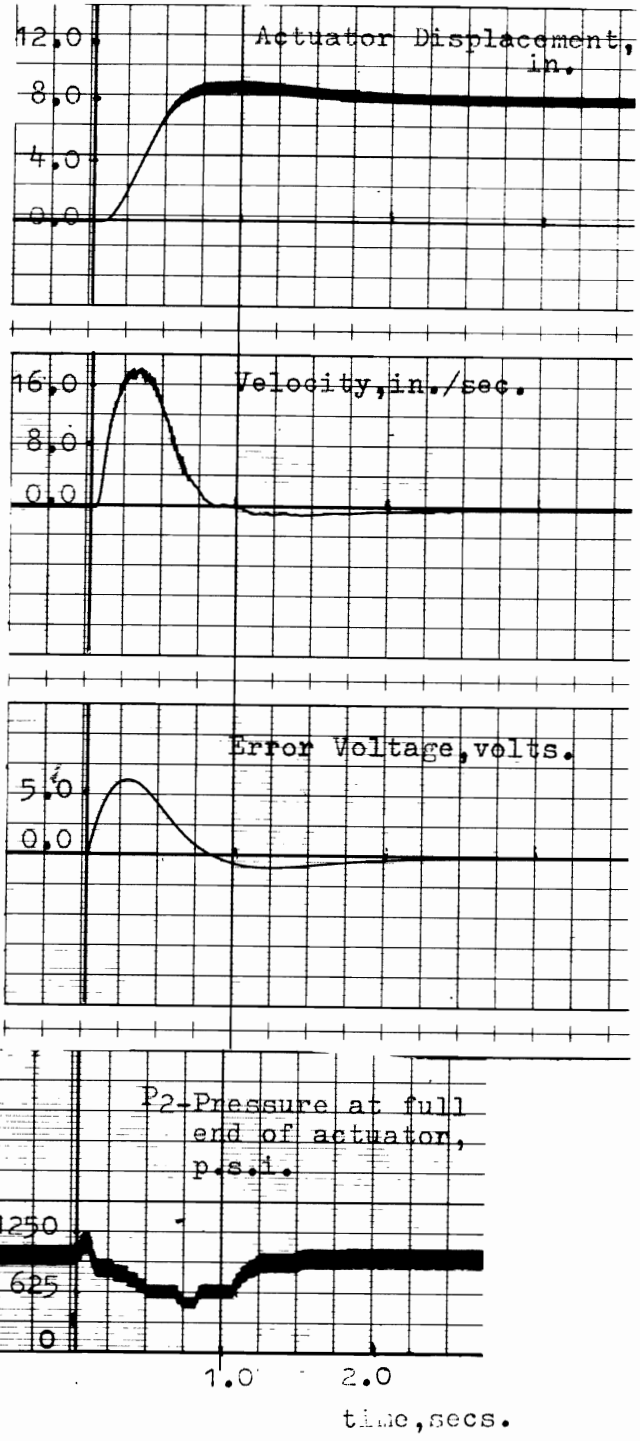

Figure 4-21 Actual System Performance for a Step Input of 2. 0 Volts - Extension

CHAPTER 5

DISCUSSION AND CONCLUSIONS

5.1 Introduction

The results presented in the last chapter indicate some variations between the mathematical model and the physical model.

Based on the assumptions made during the development of the mathematical model, some suggestions as to the possible sources for these deviations are presented in the next section and some recommendations for improving the accuracy of the model are made.

In the final section some conclusions based on the work done in this paper are presented.

5.2 Discussion

Some of the main deviations in the results are discussed hereafter:

5.2.1 The ratio of maximum velocity to maximum error voltage:

This ratio is an indication of the valve spool displacement per unit input current. From equations 3-7 and 3-16 it is seen that if $\dot{x}_v$, and hence the higher derivatives of x_v, are made zero we

get:

$$x_v = \frac{K_1}{K_w} I_s$$

As indicated in chapter 4 the spool displacement response to a step input follows the error voltage with a negligible lag. Hence at the point of maximum error voltage, $\dot{x}_v$ is assumed to be zero.

The spool displacement at this point is proportional to K_1/K_w. Also the velocity is proportional to x_v, and I_s is directly proportional to the error voltage. Hence any deviation in the determination of the actual ratio K_1/K_w can cause a deviation between the predicted value of the maximum velocity and the actual value. If the value of the feedback spring stiffness, K_w, is higher than the value specified and taken into account in the simulation, then the resulting maximum velocity will be lower.

Also, fluid inertance and resistance in the return lines can cause a reduction in the value of the maximum velocity. However, the fact that the ratio of maximum velocity to maximum error voltage becomes greater with higher step inputs and consequently higher fluid velocities in the line, tends to eliminate the fluid resistance as a cause for the observed deviation.

Another factor could be the variation of the weight component acting along the axis of the linear actuator with the actuator displacement, due to the installation geometry. In equation 3-26 the weight component was assumed constant which is applicable to small excursions. However with larger actuator displacements the weight component tends to decrease in extension and increase in retraction. Hence with larger step inputs and consequently larger displacements the weight component is higher in retraction causing higher velocities and is lower in extension so that more force is available for mass acceleration and consequently higher velocities result.

Hence it is assumed that further investigation into the characteristics of the feedback spring may provide more information as to the source of the deviation and including the weight variation with the actuator stroke in the mathematical model may improve the accuracy of the velocity prediction.

Unfortunately the available analog computer did not have enough capacity to include this variation.

5.2.2 Error Voltage :

The error voltage, and consequently the current, available at the input to the valve torque motor was higher in the test results than

in the simulation results. This is due to simplification of the RC network transfer function, again to accomodate the available computer capacity. This however had no effect on the time response of the system but caused the voltage amplitude to be multiplied by a factor of 0. 5.

5. 2. 3 Inflexion of the velocity response curve:

A variable gain circuit was introduced in the tested system reducing the gain G_a at lower voltages. This circuitry was not taken into account in the mathematical model.

5. 3 Conclusions

In the preceding chapters the following was achieved:

5. 3. 1 A mathematical model was developed for an actuator system which included the effects of spool flow forces and changing volumes.

5. 3. 2 The model was simulated on an analog computer.

5. 3. 3 Tests were conducted on the physical system and the results compared with those obtained from the simulation.

Through the results show good correlation between the simulated and actual actuator displacement, and in the general shape and time constants of the velocity, error voltage and pressure responses, the predicted ratio of maximum velocity to maximum error voltage in response to a step input deviated from the actual results. Also the predicted results of the maximum error voltage were lower than those obtained from the actual system. An explanation for probable cause of these deviations is discussed in sections 5.2.1 and 5.2.2.

Improvement in the simulation accuracy and saving in computer amplifiers can be achieved if an actual electronic circuit, taking into account the time scaling used in the simulation, is directly connected to the computer.

Also an experimental model of the system connected individually to a predetermined weight can eliminate some of the varying factors, thus providing an improved basis of comparing the simulation results. Finally, the model and the simulation provided a valuable tool in studying the trends in system performance and in a better understanding of the factors involved and their effect on the performance.

BIBLIOGRAPHY

(1) LEE, S. Y. and J. F. BLACKBURN "Contributions to Hydraulic Control 1. Steady State Axial Forces on Control Valve Piston". ASME Transactions, Volume 74, August 1952.

(2) LEE, S. Y. and J. F. BLACKBURN "Contributions to Hydraulic Control 2. Transient Flow Forces and Valve Stability" ASME Transactions, Volume 74, August 1952.

(3) BLACKBURN, J. F. "Contributions to Hydraulic Control 3. Pressure Flow Relationships for 4-way Valves " ASME Transactions, Volume 75, August 1953.

(4) BLACKBURN, J. F. "Contributions to Hydraulic Control 4. Notes on the Hydraulic Wheatstone Bridge". ASME Transactions, Volume 75, August 1953.

(5) BLACKBURN, J. F. "Contributions to Hydraulic Control 5. Lateral Forces on Hydraulic Pistons" ASME Transactions, Volume 75, August 1953.

(6) LEE, S. Y. "Contributions to Hydraulic Control 6. New Valve Configurations for High-Performance Hydraulic and Pneumatic Systems". ASME Transactions, Volume 76, August 1954.

(7) BLACKBURN, J. F., G. REETHOF and J. L. SHEARER. "Fluid Power Control". The Technology Press of M. I. T. and John Wiley and Sons, New York 1960.

(8) SHEARER, J. L. "Dynamic Characteristics of Valve Controlled Hydraulic Servomotors". ASME Transactions, Volume 76, August 1954.

(9) RAUSCH, R. G., "The Analysis of Valve - Controlled Hydraulic Servomechanism" The Bell System Technical Journal, New York, Volume 38, November 1959.

(10) FLEMING, G. K., "Analysis of Incompressible Curved Jet Flow in Control Elements". PhD Thesis presented at the University of Waterloo, October 1967.

(11) FITCH, E. C., "The Simulation of Nonlinear Characteristics in Hydraulic Servo Systems". Engineering Research Bulletin, Oklahoma State University, Publication No. 131, June 1963.

(12) SINH LE QUOC "Etudes Theorique et Experimentale d'une Servo Commande Hydraulique de Vitesse". M. Sc Thesis presented to the University of Sherbrooke, August 1968.

(13) GLICKMAN, M., "Simulation of the effects of load on hydraulic Servo Actuators" Simulation, Vol. 12, March 1969.

(14) WANG, P.K.C., "Mathematical Models for Time-Domain Design of Electrohydraulic Servomechanisms" AIEE Transactions, Volume 80, November 1961.

(15) BUTLER, R. - "A Theoretical Analysis of the Response of a Loaded Hydraulic Relay" Proceedings, Institution of Mechanical Engineers, London, England, Volume 173, No. 16, 1959.

(16) TURNBULL, D.E. "The Response of a Loaded Hydraulic Servomechanism" Proceedings, Institution of Mechanical Engineers, London, England, Volume 173, No. 9, 1959.

(17) ZABORSZKY, J. and H.J. HARRINGTON "Generalized Charts of the Effects of Nonlinearities in Electrohydraulic Control Valves" AIEE Transactions, Volume 76, May 1957.

(18) ZABORSZKY, J. and H.J. HARRINGTON "A Describing Function for the Multiple Nonlinearities Present in 2-stage Electrohydraulic Control Valves" AIEE Transactions, Volume 77, January 1958.

(19) WANG, P. K. C., "Analytical Design of Electrohydraulic Servomechanisms with Near Time - Optimal Responses" AIEE Transactions, January 1963.

(20) DAVIES, R. M., "Analytical Design for Time Optimum Transient Response of Hydraulic Servo Mechanisms" Journal of Mechanical Engineering Science, Volume 7, 1955.

(21) "Technical Bulletin 103 "Moog Servocontrols Inc., East Aurora, N. Y., January 1965.

(22) MERRITT, H. E. "Hydraulic Control Systems" John Wiley and Sons, 1967.

(23) ODIERNA, A. V., "A Synergistic Six-Degree-of-Freedom Motion System". AIAA Visual and Motion Simulation Technology Conference March 1970.

APPENDIX "A"

SPOOL FLOW FORCES

The spool flow forces consist of the steady state flow forces and the transient flow forces as explained by Lee and Blackburn (1-6). The steady state force acting on a valve spool due to flow leaving the valve chamber is described by:

$$F_{ss} = 2C_d C_v A_o (P_1 - P_2) \qquad \ldots.(A-1)$$

where C_d - discharge coefficient of spool orifice

C_v - velocity coefficient

A_o - orifice area

P_1 - pressure in valve chamber

P_2 - pressure downstream from orifice

θ - jet angle

F_{ss} - steady state flow force

θ is found to be 69° after a certain opening of the valve.

Using $C_d = .61$, $C_v = .98$, $\cos 69° = .358$

we get:

$$F_{ss} = .43W(P_1 - P_2)x_v \qquad \ldots. (A-2)$$

where W - area gradient of orifice

for our case there are two orifices in the spool.

Hence, $F_{ss} = .43WX_v(\Delta P_1 + \Delta P_2)$ $\ldots.(A-3)$

The effect of steady state flow forces is studied for the case of symmetrical loading (hydraulic motor) in a system identical with Sinh's (12).

In this case $\Delta P_1 = \Delta P_2$ and

$$\Delta P_1 + \Delta P_2 = P_s - P_L \qquad \ldots\ (A\text{-}4)$$

Where P_L is the pressure differential across the load.

Combining (A-3) and (A-4) we get:

$$F_{ss} = .43WX_v (P_s - P_L) \qquad \ldots\ (A\text{-}5)$$

which is the second term used in equation (3-9).

The transient flow force due to the acceleration or deceleration of the fluid in the annular valve chamber can be evaluated by applying Newton's second law to the mass of fluid.

$$F_T = M \cdot a = \rho LA_v \frac{d}{dt}\left(\frac{Q}{A_v}\right) = \rho L \cdot \frac{dQ}{dt}$$

where Q - volumetric flow through orifice

A_v - area of the valve land

L - axial length between incoming and outgoing flows.

but $Q = C_d W X_v \sqrt{\frac{2}{\rho}(P_1 - P_2)}$

hence

$$F_T = LC_d W \sqrt{2\rho (P_1 - P_2)}\, \dot{X}_v + \frac{LC_d W X_v}{\sqrt{\frac{2}{\rho}(P_1 - P_2)}} \frac{d}{dt}(P_1 - P_2)$$

There is little direct evidence to indicate that the pressure rate term contributes substantially to valve dynamics and therefore it is usually neglected (22).

Hence $F_t = LC_d W\sqrt{2\rho(P_1 - P_2)}\ \dot{X}_v$

designating: $C_d W \sqrt{2\rho} = K$,

we get:

$$F_T = K \cdot L \cdot \sqrt{P_1 - P_2}\ \dot{X}_v$$

or $$F_T = K \cdot L \sqrt{\Delta p}\ \dot{X}_v \qquad \ldots\ (A\text{-}6)$$

For the MOOG valve controlling an asymmetrical actuator we have two opposed orifices and the transient flow force will be studied for the following cases:

1. X_v positive: see Figure A-1

1.1 Valve opening: i.e. $\dot{X}_v$ positive

The transient force exerted by the fluid on the spool will be:

$$F_T = F_{T_1} + F_{T_2} = K \cdot L \cdot (\sqrt{\Delta p_2} - \sqrt{\Delta p_1})\ \dot{X}_v$$

F_{T_1} and F_{T_2} are in the direction of the reaction to the accelerating fluid and are indicated by the full arrows in Figure A-1. As Δp_2 is always greater than Δp_1 due to the higher flow across the same orifice area, the transient force will be in the positive force direction as indicated in Figure A-1

1.2 Valve Closing: i. e. $\dot{X}_v$ negative.

The transient force will be $F_T = F_{T_1} + F_{T_2}$. The directions of F_{T_1} and F_{T_2} are indicated by the broken arrows in Figure A-1. They are in the direction of the reaction to the decelerating fluid.

$$F_T = K \cdot L \left(\sqrt{\Delta p_1} - \sqrt{\Delta p_2}\right) \left|\dot{X}_v\right|$$

and hence

$$F_T = K \cdot L \left(\sqrt{\Delta p_2} - \sqrt{\Delta p_1}\right) \dot{X}_v$$

(In this case $\dot{X}_v$ was negative)

2. X_v negative

2.1 Valve closing:

In this case the valve closing direction coincides with the positive $\dot{X}_v$ direction. Hence $\dot{X}_v$ is positive.

F_{T_1} and F_{T_2} are in the direction of the reaction to the decelerating fluid and are shown by the full arrows in Figure A-2.

$$F_T = F_{T_1} + F_{T_2} = K \cdot L \left(\sqrt{\Delta p_1} - \sqrt{\Delta p_2}\right) \dot{X}_v$$

or $$F_T = - K \cdot L \left(\sqrt{\Delta p_2} - \sqrt{\Delta p_1}\right) \dot{X}_v$$

2.2 Valve opening

In this case the valve opening direction coincides with the negative X_v direction. Hence $\dot{X}_v$ is negative.

The directions of F_{T_1} and F_{T_2} are indicated by the broken arrows in Figure A-2 which represents the direction of the reaction to the accelerating fluid.

$$F_T = F_{T_1} + F_{T_2} = K \cdot L \left(\sqrt{\Delta P_2} - \sqrt{\Delta P_1}\right) \dot{X}_v$$

or $$F_T = - K \cdot L \left(\sqrt{\Delta P_2} - \sqrt{\Delta P_1}\right) \dot{X}_v$$

We conclude that the value of the transient flow force term in equation (3-9) can be positive or negative according to $\dot{X}_v$ but the sign preceding it is dependent on X_v only. It will be positive for positive X_v and vice versa.

The effect of the transient and steady state forces was evaluated for the case of symmetrical loading (hydraulic motor) in a system identical with Sinh's (20). In this case we would have $\Delta P_1 = \Delta P_2$, for all conditions, based on the assumptions made in section 3.1, as the flow is equal across the equal orifices area.

Hence for a symmetrical spool with equal L the transient forces F_{T_1} and F_{T_2} will cancel each other. To test the effect of the force, however, a difference in the length L was assumed. Designating that difference by ΔL we arrive at the form used in equation (3-9):

$$F_T = C_d \sqrt{2\rho}\, W \Delta L \sqrt{\Delta P}\, \dot{X}_v$$

The model including the terms for the flow forces was run on the analog computer and the responses of x_v and x_f were recorded. The terms were then removed from the model which was then run with otherwise identical parameters. The results were compared and found to have insignificant differences.

These terms were then removed from the final model, adding to its simplification.

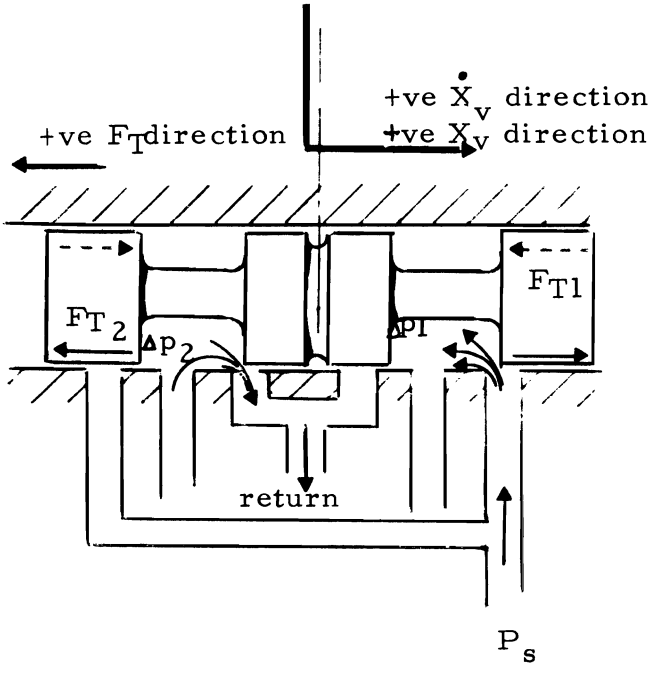

Figure A-1 X_v Positive

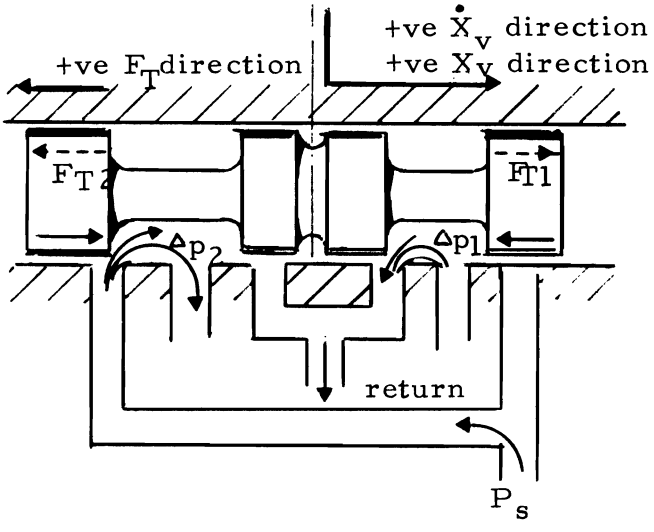

Figure A-2 X_v Negative

APPENDIX "B"

DERIVATION OF EQUATIONS (3-11), (3-17) AND (3-19)

The derivation of the equation for the rate of change of pressure of a compressible fluid starts with the definitions of the volume rate of flow, and the fact that density is a function of time only i. e.

$$Q = \frac{1}{\rho}\dot{m} = \frac{1}{\rho}\frac{d}{dt}(\rho v) = \dot{v} + \frac{v}{\rho}\dot{\rho} \qquad \ldots\ (B\text{-}1)$$

where:

Q = volume rate of flow

$\dot{m}$ = rate of change of mass of fluid within the chamber (control volume)

v = volume of the hydraulic fluid

ρ = density of hydraulic fluid

also the bulk modulus for a compressible fluid is defined to be:

$$\beta = -v\frac{dP}{dv}\Bigg|_{\text{mass = const.}}$$

where:

dv = the decrease in volume of the fluid

dp = the increase in pressure to the fluid

v = the original volume of the fluid

By using the above definitions the following equation holds

$$\dot{\rho} = \frac{\rho}{\beta}\dot{P} \qquad \ldots\ (B\text{-}3)$$

Substituting equation (B-3) into equation (B-1):

$$Q = \dot{v} + \frac{v}{\beta}\dot{P} \qquad \ldots\ (B-4)$$

However the rate of change of the volume of fluid, assuming no cavitation exists can be written as:

$$Q = \dot{v} = A \cdot \dot{y} \qquad \ldots\ (B-5)$$

where $\dot{y}$ = actuator or spool velocity as applicable

A = area of actuator or spool

If a laminar type leakage flow is assumed from the high pressure chamber to the low pressure chamber an additional flow occurs:

$$Q_\ell = C_\ell \ (P_1 - P_2) \qquad \ldots\ (B-6)$$

where Q_ℓ = leakage flow

C_ℓ = leakage coefficient

P_1 = pressure in the higher pressure chamber

P_2 = pressure in the lower pressure chamber

From (B-4), (B-5) and (B-6) equations (3-17) and (3-19) result.

For equation (3-11) we define Q_{L_v} as the average flow in and out of the two spool end chambers P_{L_v} as the difference in pressure between the two end chambers and V_v as the total volume in the two end chambers with the spool in mid position.

The flow into the higher pressure chamber according to (B-4) and (B-5) is:

$$Q_{v_1} = A_v \dot{x}_v + \frac{V_1}{\beta}\dot{P}_1 + C_\ell (P_1 - P_2)$$

The flow from the lower pressure chamber is

$$Q_{v_2} = A_v \dot{x}_v - \frac{V_2}{\beta} \dot{P}_2 + C_\ell (P_1 - P_2)$$

also the volumes of the higher and lower pressure chambers are:

$$V_1 = V_o + A_v \cdot x_v$$

$$V_2 = V_o - A_v \cdot x_v$$

where V_o volume of each chamber with spool in mid position

hence:

$$V_v = V_1 + V_2 = 2V_o$$

and with $Q_{L_v} = \frac{Q_{v_1} + Q_{v_2}}{2}$

we get:

$$Q_{L_v} = A_v \dot{x}_v + \frac{V_o}{2\beta} (\dot{P}_1 - \dot{P}_2) + C_\ell P_{L_v} + \frac{A_v \cdot x_v}{2\beta} (\dot{P}_1 + \dot{P}_2)$$

The spool is a symmetrical load hence

$$P_s = P_1 + P_2$$

where P_s = supply pressure to the nozzles which is identical to system supply pressure and is assumed to be constant.

Hence: $\dot{P}_1 + \dot{P}_2 = o$

and

$$Q_{L_v} = A_v \dot{x}_v + \frac{V_v}{4\beta} \dot{P}_{L_v} + C_\ell P_{L_v}$$

which is equation (3-11).

APPENDIX "C"

NUMERICAL VALUES OF THE PARAMETERS

PARAMETER	VALUE
A_1	3.40 in^2
A_2	8.29 in^2
A_v	.1104 in^2
B_m	10 lb. sec/in.
C_l	.6 x 10^{-3} in^5 /sec. lb
$C_d\sqrt{2/\rho}$	104.5 $in^2/\sqrt{lb.}$ - sec
G_a	6.0
G_f	.278 volt/in.
K_1	.031 in. lb./mA
K_2	187.0 in^3/sec/in.
K_f	90.0 in. lb/in.
K_w	2.4 in. lb/in.
M	16.6 lb. sec^2/in.
P_s	1500 p.s.i.
R_v	668.1 ohms
RC	.34 secs.
V_{t_1}	106.7 in^3
V_{t_2}	245.0 in^3
w	2.36 in
W	6400 lbs
ω_n	4580 rad/sec

PARAMETER	VALUE
ζ_n	.4
ω_h	1940 rad/sec
δ_h	1.0
β	1.0×10^5 lb/in^2

APPENDIX "D"

EQUATIONS SCALING AND ANALOG PATCHING

The following maximum values of the variables were determined from the known performance of the physical system and by the coefficient values:

variable	maximum value	units
$\dot{P}_1$	10^6	psi/sec
$\dot{P}_2$	10^6	psi/sec
P_1	2000	psi
P_2	2000	psi
$\ddot{y}$	2000	in./sec^2
$\dot{y}$	60	in./sec
y	30	in.
$\ddot{x}_f$	10^5	in./sec^2
$\dot{x}_f$	10	in./sec
x_f	.010	in.
$\dddot{x}_v$	10^8	in./sec^3
$\ddot{x}_v$	10^4	in/sec^2
$\dot{x}_v$	10	in./sec
x_v	.100	in.
E_i	10	Volts
E_o	10	Volts

variable	maximum value	units
$\dot{E}_o$	10	Volts/sec
I_s	10	mA

The following are the transformed equations from section 4.2:

$$\left[\frac{\ddot{x}_f}{10^5}\right] = -\frac{2\omega_n \zeta_n}{10^4}\left[\frac{\dot{x}_f}{10}\right] - 10\left(\frac{\omega_n^2}{10^8}\right)\left[100\, x_f\right]$$

$$-\frac{K_w}{K_f}\frac{\omega_n^2}{10^6}\left[10\, x_v\right] + \frac{K_1}{K_f}\frac{\omega_n^2}{10^4}\, 1.5\left[\frac{I_s}{15}\right]$$

$$\left[\frac{\ddot{x}_v}{10^8}\right] = \frac{K_2}{A_v}\frac{\omega_h^2}{10^{10}}\left[100\, x_f\right] - \frac{2\delta_h\omega_h}{10^4}\left[\frac{\ddot{x}_v}{10^4}\right] - \frac{\omega_h^2}{10^7}\left[\frac{\dot{x}_v}{10}\right]$$

$$\left[\frac{\ddot{y}}{2000}\right] = \frac{A_1}{M}\left[\frac{P_1}{2000}\right] - \frac{A_2}{M}\left[\frac{P_2}{2000}\right] - \frac{3B_m}{100M}\left[\frac{\dot{y}}{60}\right] + \frac{g}{2000}$$

$$\frac{\dot{P}_1}{10^6} = 10\,\frac{\beta C_d w\sqrt{\frac{2}{\rho}}}{10^7 V_{t_1}}\cdot\sqrt{20}\,\left[10\, x_v\right]\sqrt{\left[\frac{\Delta P_1}{2000}\right]}$$

$$-\frac{6A_1\beta}{10^5 V_{t_1}}\left[\dot{y}/60\right] - \frac{2C_\ell\,\beta}{10^3 V_{t_1}}\left[\frac{P_1 - P_2}{2000}\right]$$

$$\frac{\dot{P}_2}{10^6} = -\frac{\beta C_d \sqrt{2/\rho}\, w}{10^6 V_{t_2}} \sqrt{20}\left[10x_v\right]\sqrt{\left[\frac{\Delta P_1}{2000}\right]}$$

$$+\frac{6A_2\beta}{10^5 V_{t_1}}\left[\dot{y}/60\right] + \frac{2C_\ell\,\beta}{10^3 V_{t_2}}\left[\frac{P_1 - P_2}{2000}\right]$$

$$\left[\frac{\dot{E}_o}{10}\right] = \left[\frac{V_i}{10}\right] - 3\,G_f\left[\frac{y}{30}\right] - \frac{1}{RC}\left[\frac{E_o}{10}\right]$$

$$\left[\frac{I_s}{15}\right] = \frac{10^3 G_a}{1.5\,R_v}\left[\frac{E_o}{10}\right]$$

With the time scaling chosen as α = 1000, the analog patching is as shown in Figures D-1 and D-2. The pot values are as shown in the table below:

POT	VALUE	QUANTITY
P01	.1030	$\beta C_d w \sqrt{2/\rho \cdot 20} / 10^7 V_{t_1}$
P02	.5000	$10^6/2000\alpha$
P05	.5600	$K_w \omega^2_n / 10^6 K_f$
P06	.7500	$P_s/2000$

POT	VALUE	QUANTITY
P07	.0011	$2C_{\ell}\beta / 10^3 V_{t_1}$
P08	.0010	$1 / \alpha$
P12	.0003	$2C_{\ell}\beta / 10^3 V_{t_2}\ \alpha$
P15	.3760	$\omega_h^2 / 10^7$
P31	.8150	$3G_f$
P32	.1000	$100/\alpha$
P36	.1980	$g/2000$
P38	.3880	$2\delta_h \omega_h / 10^4$
P40	.2050	A_1/M
P60	.0020	$2/\alpha$
P62	.0180	$3B_m/100M$
P65	.0333	$100/3\alpha$
P66	.1017	$6A_2\beta / 10^5 V_{t_2} \cdot 10^3 / 2\alpha$
P67	.0500	$A_2/10M$
P68	.1915	$6A_1\beta / 10^5 V_{t_1}$
P70	.2240	$C_d w \sqrt{2/\rho}\ \beta\sqrt{20} / 10^6 V_{t_2} \cdot 10^3 / 2\alpha$
P90	.6500	$\frac{1}{10} K_1 \omega_n^2 / 10^4 K_f \cdot 10^3 G_a / R_v$
P96	.3680	$2\zeta_n \omega_n / 10^4$
P100	.2098	$\omega_n^2 / 10^8$
P101	.6375	$K_2 \omega_h^2 / 10^{10} A_v$
Q04	Variable	$V_i/10$
Q09	.0029	$1/\alpha RC$
Q14	.3860	$W/2000A_2$, I.C. for $[P_2/2000]$

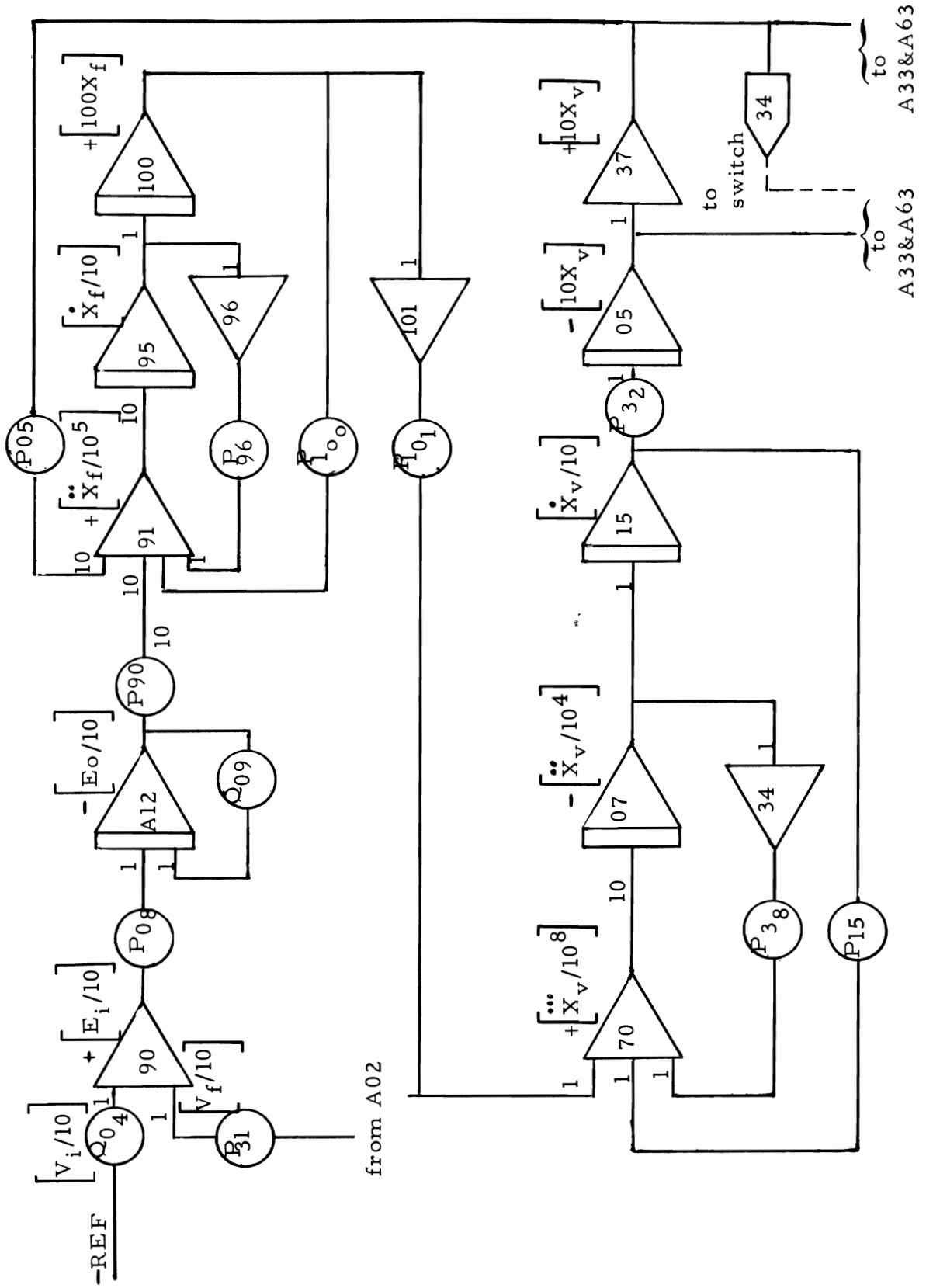

Figure D-1 Analog Patching - Servo Valve

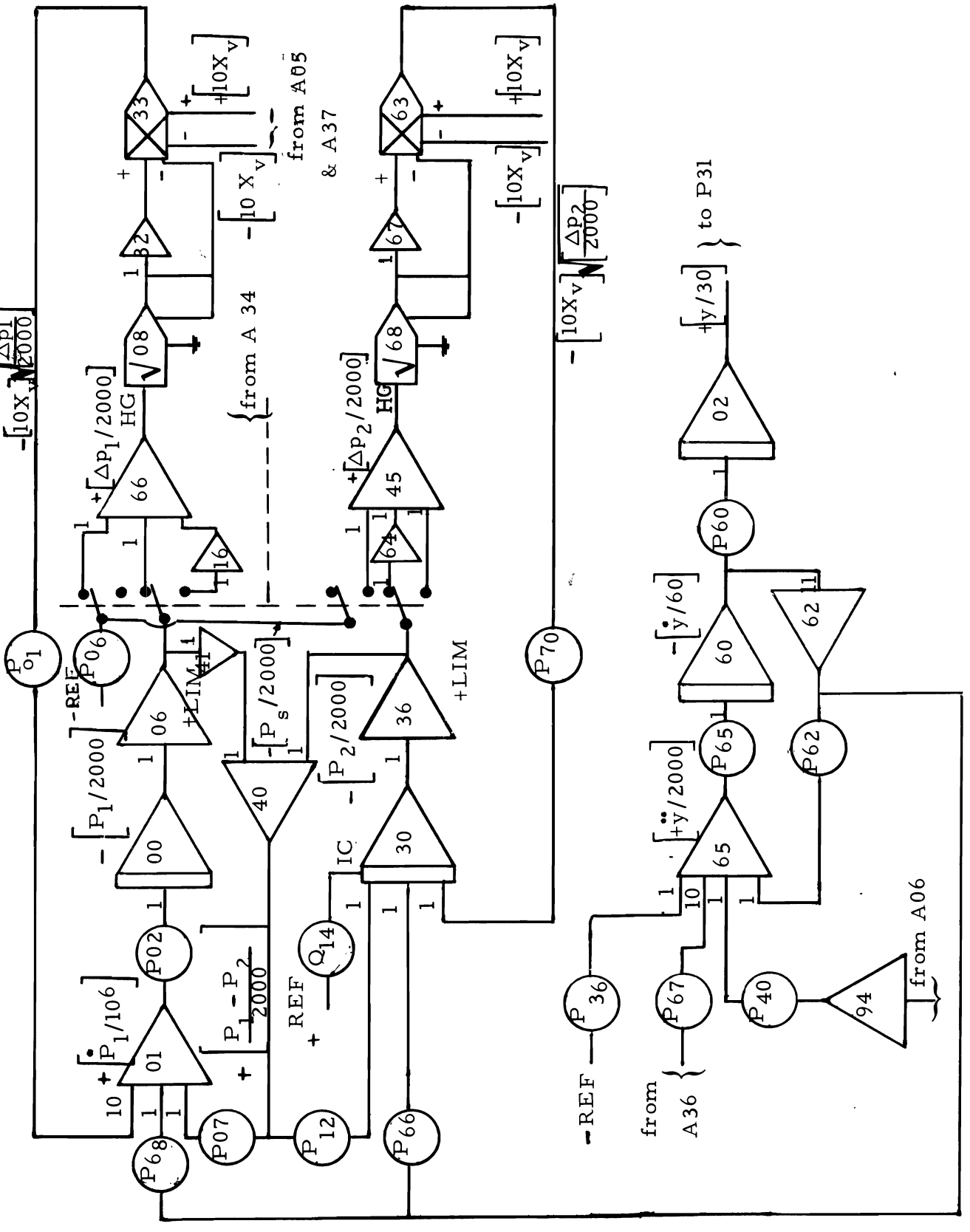

Figure D-2 Analog Patching - Load

APPENDIX "E"

NOMENCLATURE

SYMBOL	DEFINITION
A_1	Actuator rod end area, in^2.
A_2	Actuator full end area, in^2.
A_v	Valve spool end area, in^2.
B_a	Armature damping factor, in. lb. sec/rad.
B_m	Damping coefficient of actuator, lb. sec/in.
C_l	Actuator leakage coefficient, in^5/sec. lb.
C_d	Orifice discharge coefficient, non dimensional
C_{t_s}	Spool leakage coefficient, in^5/sec. lb.
E_o	Error voltage, output from RC network, volts.
G_a	Forward gain, non dimensional
G_f	Feedback Gain, volt/in.
I_s	Input current to valve, mA
J_a	Rotational inertia of armature/flapper, in lb/sec^2
K_a	Torsion spring constant of armature, in. lb/rad.
K_1	Torque motor gain, in. lb/mA
K_m	Magnetic spring constant of torque motor, in. lb./ rad.
K_2	Flapper nozzle flow gain, in^3/sec/in.
K_f	Net stiffness of armature/flapper, in. lb./in.
K_w	Feedback wire stiffness, in. lb/in.

SYMBOL	DEFINITION
K_{c_e}	Flapper nozzle flow pressure coefficient $in^5/sec.$ lb.
M	Actuator load mass, lb. $sec^2/in.$
M_v	Valve spool mass, lb. $sec^2/in.$
P_1	Pressure in the actuator rod end chamber, lb/in^2
P_2	Actuator full end chamber pressure, lb/in^2
P_s	Supply pressure, lb/in^2
P_L	Pressure differential across valve spool, lb/in^2
Q_ℓ	Leakage flow across actuator, in^3/sec
Q_1	Flow to rod end chamber, in^3/sec
Q_2	Flow from full end chamber, in^3/sec
Q_{L_v}	Average flow to valve spool end volume, $in^3/sec.$
R_v	Electrical resistance of valve and circuit, ohms
RC	Time constant of RC network, secs.
T_d	Torque developed by valve motor, in. lb.
V_{t_1}	Rod end volume at mid stroke, including piping, $in^3.$
V_{t_2}	Full end volume at mid stroke, including piping, $in^3.$
V_v	Valve spool end volume, $in^3.$
w	Valve spool area gradient, in.
W	Actuator load weight, lbs.

SYMBOL	DEFINITION
x_f	Flapper displacement from null, in.
x_v	Valve spool displacement from null, in.
θ	Angular displacement of armature, rad.
ρ	Fluid density, lb sec^2/in^4.
β	Fluid bulk modulus of elasticity, lb/in^2.
ω_n	Natural frequency of first stage, rad/sec.
ζ_n	Damping factor of first stage, non dimensional
ω_h	Natural frequency of second stage, rad/sec.
δ_h	Damping factor of second stage, rad/sec.